From DEPARTMENT OF CLINICAL NEUROSCIENCE
Karolinska Institutet, Stockholm, Sweden

INTERACTIONS BETWEEN THE OPIOID AND SEROTONIN SYSTEMS IN CHRONIC PAIN. QUANTITATIVE LIVE CELL STUDY BY FLUORESCENCE CROSS-CORRELATION SPECTROSCOPY (FCCS)

Vlad Radoi

Karolinska Institutet

Stockholm 2019

Published by Karolinska Institutet.
Printed by EPrint AB 2019

ISBN 978-91-7831-620-5

INTERACTIONS BETWEEN THE OPIOID AND SEROTONIN SYSTEMS IN CHRONIC PAIN. QUANTITATIVE LIVE CELL STUDY BY FLUORESCENCE CROSS-CORRELATION SPECTROSCOPY (FCCS)
THESIS FOR DOCTORAL DEGREE (Ph.D.)

By

Vlad Radoi

Principal Supervisor:
Associate Professor Vladana Vukojević
Karolinska Institutet
Department of Clinical Neuroscience

Co-supervisor(s):
Professor Eva Kosek
Karolinska Institutet
Department of Clinical Neuroscience

Professor Camilla Svensson
Karolinska Institutet
Department of Physiology and Pharmacology

Professor Lars Terenius
Karolinska Institutet
Department of Clinical Neuroscience

Mentor:
Dr. André Orlieb Guerreiro-Cacais
Karolinska Institutet
Department of Clinical Neuroscience

Opponent:
Professor Dominique Massotte
CNRS Strasbourg
Department of Cellular and Integrative Neuroscience

Examination Board:
Professor Jerker Widengren
Royal Institute of Technology (KTH)
Department of Quant- and biophotonics

Professor Ernst Brodin
Karolinska Institutet
Department of Physiology and Pharmacology

Professor Joëlle Rüegg
Uppsala University
Department of Organismal Biology, Environmental Toxicology

This PhD thesis is dedicated to the love of my life Jonas. You have been a pillar of support, compassion, empathy and encouragement throughout this process. You have helped me celebrate achievements and tolerated me at my absolute worst. Without you, this would not have been possible! Te iubesc Veveriţă!

ABSTRACT

Chronic pain is a major health issue worldwide. It enacts considerable suffering on the affected individuals and significantly increases the societal burden, as it is the most common reason why individuals seek sick leave and ask for medical help. Pharmacotherapies for chronic pain are not satisfactory, and many patients, despite taking medications, do not find relief and end up using opioids. Long-term opioid use carries with it numerus adverse effects, including but not limited to opioid induced hyperalgesia (OIH), tolerance, dependence (addiction) and opioid-related deaths. OIH is defined as a state of nociceptive sensitization, *i.e.* a state of becoming more sensitive to painful stimuli when using opioids for a long time. Cellular and molecular mechanisms that underlie OIH are still not fully understood, and efficient treatment strategies that retain the analgesic effects of opioids, while reducing this negative side effect are therefore underdeveloped.

Clinical studies in healthy subjects and patients with fibromyalgia, a chronic pain syndrome with abnormalities in cerebral opioid signaling, have implicated interactions between the mu-opioid (MOP) and the serotonin 1A (5-HT_{1A}) receptors in descending pain modulatory circuits as important for chronic pain modulation. Preclinical studies have shown that co-treatment with 5-HT_{1A} agonists reduces OIH, diminishes the rewarding effects of morphine and the development of opioid tolerance. They have also provided indirect evidence for the co-localization of MOP and 5-HT_{1A} receptors in the same nerve terminals, and demonstrated that MOP and 5-HT_{1A} synergistically inhibited GABA release in the periaqueductal gray (PAG), a structure that mediates opioid-based pain control. Based on these findings, it was proposed that MOP and 5-HT_{1A} heterodimerization is a potential mechanism through which MOP- and 5-HT_{1A}-mediated signaling pathways are interlinked. It is further hypothesized that MOP and 5-HT_{1A} heterodimer formation alters cellular signaling and contributes to neuroplastic changes that, eventually, lead to sensitization of pronociceptive pathways at the organism level. However, while co-localization of MOP and 5-HT_{1A} receptors in discrete brain and spinal cord regions is well documented, the existence of heterodimers between MOP and 5-HT_{1A} receptors has, thus far, only been shown in one study, which relied on the use of co-immunoprecipitation and Bioluminescence Resonance Energy Transfer (BRET) to demonstrate that these heterodimer complexes could form.

The primary objective of my PhD studies was to challenge the hypothesis that prolonged exposure to non-peptide opioids promotes heterodimer formation between MOP and 5-HT_{1A} receptors, and that this effect can be abolished by co-treatment with 5-HT_{1A} agonists. To this aim, cell lines of human and rat origin where genetically transformed to stably express

physiologically relevant levels of MOP and 5-HT_{1A} receptors tagged with spectrally distinct fluorescence reporters. Fluorescence Cross-Correlation Spectroscopy (FCCS), the dual color variant of the quantitative and nondestructive analytical technique called Fluorescence Correlation Spectroscopy (FCS), was used to characterize the receptor-receptor interactions in live cells. Additionally, confocal laser scanning microscopy (CLSM) was used to map the consequences of non-peptide opioid treatment on Ca^{2+} signaling dynamics and western blotting was applied to investigate signaling cross-talk *via* mitogen-activated protein kinases (MAPKs) p38 and the extracellular signal-regulated kinase (ERK1/2).

The work presented in this thesis, summarized in papers I-V, has contributed to better understanding of important basic cellular and molecular mechanisms that underlie signal transduction and material uptake across the plasma membrane. In particular, the work presented in papers I-III focuses on cellular and molecular mechanisms that underlie the development of OIH. In **Paper I**, we have shown that prolonged exposure to non-peptide opioids facilitates heterodimer formation between MOP and 5-HT_{1A} receptors in live cells expressing physiologically relevant receptor levels. The extent of receptor heterodimerization was found to be both, opioid-specific and dose-dependent. Furthermore, we have shown that different opioids differently affected second messenger pathways, as indicated by differences in Ca^{2+} signaling dynamics and differential activation of p38 and ERK1/2 MAPKs. In **Paper II**, we have shown that 5-HT_{1A} agonists such as buspirone and three newly identified buspirone analogs: B2, B3 and B5, can effectively reverse MOP–5-HT_{1A} heterodimerization, thus counteracting the aversive effects of morphine. Importantly, this study, which brought together molecular modeling, virtual screening and advanced experimental tests in live cells, may in the future lead to the development of new drugs that target MOP and 5-HT_{1A} heterodimer formation. In **paper III**, we have quantitatively characterized using FCS/FCCS and PhotoActivated Localization Microscopy (PALM) the nanoscale lateral dynamics and spatial organization of wild type MOP and its naturally occurring isoform (MOP_{N40D}). We have shown that this non-synonymous single-nucleotide polymorphism (SNP) in the *OPRM1* gene encoding the MOP, which is known to confer pain- and substance abuse-specific phenotypes at the organism level, significantly affected the lateral dynamics and organization of MOP_{N40D} at the nanoscale level. In particular, we found that MOP-containing domains were larger and more densely populated than the MOP_{N40D} harboring domains, with a small fraction of molecules residing outside of nanodomains. The opposite was found for MOP_{N40D}. Moreover, we found that cholesterol depletion dynamically regulated the partitioning of MOP but not of MOP_{N40D}, and observed that MOP and MOP_{N40D} differ with respect to opioid peptide-induced internalization, with MOP being readily internalized together with the opioid peptide upon

stimulation with β-endorphin, whereas MOP_{N40D} showed lower internalization propensity and was typically not internalized together with the opioid peptide. These apparently subtle differences at the nanoscale level may, at least in part, explain why differences with respect to opioid dependence and analgesia are observed at the organism level.

Papers IV and V describe collaborative work where CLSM and/or FCS/FCCS were used to characterize translocation across the plasma membrane and cellular uptake. In **Paper IV**, we focus on substance delivery using cell-penetrating peptides as a vehicle. Using FCS/FCCS, we revealed the heterogeneity underlying self-assembly of cell-penetrating peptides and oligonucleotides, in this case small interfering RNA (siRNA), into large molecular complexes. We showed that peptide monomers, peptide self-aggregates and polydisperse peptide/cargo complexes coexist in solution and in live cell plasma membrane, which could explain why diverse cellular uptake mechanisms were simultaneously observed for cell-penetrating peptides-based delivery of cargo molecules. In **Paper V**, CLSM imaging was used to examine the role of α-Gal carbohydrate on protein uptake and degradation by immature monocyte-derived dendritic cells (iMDDCs), as a potential cellular and molecular mechanisms underlying the development of allergy to red meat. CLSM imaging revealed that presence of allergenic α-Gal epitopes on the protein surface significantly increases the uptake of the investigated model antigens, BSA-α-Gal and HSA-α-Gal, by *in vitro* cultured human iMDDCs, and showed that the taken up proteins are processed in endosomes.

ABSTRAKT

Kronisk smärta är ett viktigt hälsoproblem världen över. Det orsakar inte bara lidande för de drabbade, utan orsakar även stora samhällsekonomiska belastningar då det är den vanligaste orsaken till sjukfrånvaro och läkarbesök. Behandlingar för kronisk smärta är sällan tillfredsställande och många patienter finner inte lindring trots första linjens medicinering, vilket resulterar i behandling med opiater. Långtidsbehandling med opiater bär med sig ett flertal ogynnsamma effekter som opioidinducerad hyperalgesi (OIH), tolerans, beroende samt opioidrelaterade dödsfall. OIH definieras som ett tillstånd av nociceptiv sensibilisering (ett tillstånd av ökad känslighet för smärtsamma stimuli) till följd av långtids opioidbruk. De cellulära och molekylära mekanismer som underligger OIH är ännu inte fullt klargjorda, således är effektiva behandlingsstrategier som bibehåller den analgetiska effekten av opioider samt minimerar deras biverkningar underutvecklade.

Kliniska studier på friska subjekt samt patienter med fibromyalgi (ett kroniskt smärtsyndrom med abnormal cerebral opioidsignalering) har påvisat interaktioner mellan mu-opioidreceptorn (MOP) och serotonin-1A-receptorn (5-HT_{1A}) i nedåtgående smärtmodulering som viktiga inom kronisk smärtmodulering. Prekliniska studier har visat att sambehandling med 5-HT_{1A}-agonister och opioider reducerar OIH, minskar de belönande effekterna hos morfin samt utvecklingen av tolerans. Dessa studier har också indirekt påvisat att MOP och 5-HT_{1A} samlokaliserar i samma nervterminaler, samt demonstrerat att MOP och 5-HT_{1A} synergistiskt hämmar GABA-utsöndring i det periakveduktala grå substansen (PAG), en struktur som medierar opioidbaserad smärtkontroll. Utifrån dessa rön har det föreslagits att heterodimerisering mellan MOP och 5-HT_{1A} är en möjlig mekanism genom vilken MOP-5-HT_{1A}-medierad signalering är sammankopplad. Det är vidare hypotetiserat att heterodimerisering mellan MOP och 5-HT_{1A} förändrar cellulär signalering och bidrar till neuroplastiska förändringar som slutligen leder till sensibilisering av pronociceptiva banor på organismnivå. Även om samlokalisationen av MOP och 5-HT_{1A} i diskreta delar av hjärnan och ryggraden är väldokumenterade så har endast en tidigare studie lyckats påvisa heterodimerisering mellan MOP och 5-HT_{1A}. Studien förlitade sig på metoderna samimmunoprecipitation och bioluminescence resonance energy transfer (BRET) för att påvisa bildningen av heterodimerer.

Det huvudsakliga målet för mina doktorandstudier var att undersöka hypotesen att långvarig exponering för ickepeptida opioider främjar bildandet av heterodimerer mellan MOP och 5-HT_{1A} och att denna effekt kan omvändas via sambehandling med 5-HT_{1A}-agonister. För detta ändamål har cellinjer med ursprung från både människa och råtta genetiskt omvandlats för

att uttrycka fysiologiskt relevanta nivåer av både MOP och 5-HT_{1A}, märkta med spektralt distinkta fluoroforer. Tvåfärgsvarianten av den kvantitativa och oförstörande analysmetoden fluorescence correlation sprectroscopy (FCS), känd som fluorescence cross-correlation spectroscopy (FCCS), var tillämpad för att karakterisera interaktionerna mellan de två receptorerna i levande celler. Konfokal laserskanningsmikroskopi (CLSM) användes för att kartlägga effekten av dessa interaktioner på kalciumsignalering, medan analys via Western Blot användes för att undersöka signalöverförning (cross-talk) via mitogenaktiverade proteinkinaser (MAPKs), p38, samt extracellulärt signalregulerande kinas (ERK1/2).

Arbetet som presenteras i denna avhandling (sammanfattat i publikationerna I-V) har bidragit till en bättre förståelse av viktiga grundläggande cellulära och molekylära mekanismer. Det arbete som presenteras publikationerna I-III fokuserar på de cellulära och molekylära mekanismer bakomliggande utvecklingen av OIH. I **publikation I** påvisar vi att långvarig exponering för icke-peptida opioider främjar bildandet av heterodimerer mellan MOP och 5-HT_{1A}, i celler som uttrycker fysiologiskt relevanta nivåer av receptorerna. Utsträckningen av receptorheterodimeriseringen påvisades vara både beroende av opioidtyp och -dos. Utöver det kunde vi påvisa att olika opioider påverkade second messenger signaltransduktionsvägar olika, då de påverkade kalciumsignalering, p38, och ERK1/2 olika. I **publikation II** visade vi att 5-HT_{1A}-agonister, så som buspiron och tre nyligen identifireade buspironanaloger (B2, B3, och B5), hade omvänd effekt på MOP-5-HT1A-heterodimerisering och således motverkade morfininducerad heterodimerisering. Denna studien band samman molekylärmodelering , virtuell undersökning och avancerade experimentella försök i levande celler. Den kan i framtiden vara gynnsamt för utvecklingen av nya läkemedel riktade mot MOP-5-HT1A-heterodimerisering. I **publikation III** har vi kvantitativt karakteriserat den spatiala organisationen av MOP och den naturligt förekommande isoformen MOP_{N40D} via FCS/FCCS och PhotoActivated Localization Microscopy (PALM) och påvisat att dessa egenskaper är viktiga determinanter för opioidreceptorers funktion. Vi fann att denna punkt mutation (single-nucleotide polymorphism) i *OPRM1* genen, som kodar för MOP, ändrade den laterala dynamiken och organisationen hos MOP_{N40D}, på ett signifikat vis. I synnerhet fann vi att MOP-berikade domäner var betydligt mer tätbefolkade än domäner som innehöll MOP_{N40D}, med en bråkdel av molekylerna utanför dessa domäner. Det motsatta visade sig gälla för MOP_{N40D}. Tömning av kolesterol regelerade dyamiskt fördelnignen av MOP, men inte av MOPN40D. Dessa subtila skillnader på nanonivå kan förklara varför signifikanta skillnader i opioid beroende och analgesi kan ses på organismnivå. I **publikation IV** tillämpades FCS/FCCS för att påvisa den heterogena naturen av cellpenetrerande peptiders samt nukleotiders (siRNA i detta fallet) självuppbyggande. Vi visade att

peptidmonomerer, peptid självaggregerade och polydispersiva peptid/frakt komplex existerade samtidigt i lösning samt i cellers plasmamembran, vilket kunde till viss del förklara varför olika upptagningsmekanismer hos cellern kunde noteras vid cellpenetrerande peptidbaserad leverans av fraktmolekyler. I **publikation V** undersökte vi de cellulära och molekylära mekanismerna bakom köttallergi, med fokus på kolhydraten α-Gals roll i proteinupptag och nedbrytning i immature monocyte-derived dendritic cells (iMDDCs). CLSM visade att α-Gal-epitopen på proteiners yta signifikant ökade upptaget av de undersökta modellallergenerna BSA-α-Gal och HSA-α-Gal i odlade humana iMDDCs och att de upptagna allergenerna bearbetas i endosomer.

LIST OF SCIENTIFIC PAPERS

I. **Vlad Radoi**, Gerd Jakobsson, Vinko Palada, Henrik Druid, Lars Terenius, Eva Kosek and Vladana Vukojević. Opioids differ in their capacity to induce heterodimer formation between the mu-opioid and the serotonin 1A receptors.
II. **Vlad Radoi**, Dimitar A. Dobchev, Vinko Palada, Mati Karelson, Eva Kosek and Vladana Vukojević. Busprione and its newly synthesized analogs hinder morphine induced heterodimer formation between the mu-opioid and the serotonin 1A receptors - A potentially new treatment strategy for opioid-induced hyperalgesia in chronic pain.
III. Rogacki MK, Golfetto O, Tobin SJ, Li T, Biswas S, Jorand R, Zhang H, **Radoi V**, Ming Y, Svenningsson P, Ganjali D, Wakefield DL, Sideris A, Small AR, Terenius L, Jovanović-Talisman T, Vukojević V. Dynamic lateral organization of opioid receptors (kappa, mu(wt) and mu(N40D)) in the plasma membrane at the nanoscale level. Traffic (Copenhagen, Denmark) 2018;19(9):690-709.
IV. Vasconcelos L, Lehto T, Madani F, **Radoi V**, Hallbrink M, Vukojevic V, Langel U. Simultaneous membrane interaction of amphipathic peptide monomers, self-aggregates and cargo complexes detected by fluorescence correlation spectroscopy. Biochim Biophys Acta Biomembr 2018;1860(2):491-504.
V. Krstić Ristivojević M, Grundström J, Tran TAT, Apostolović D, **Radoi V**, Starkhammar M, Vukojević V, Ćirković Veličković T, Hamsten C, van Hage M. α-Gal on the protein surface affects uptake and degradation in immature monocyte derived dendritic cells. Scientific Reports 2018;8(1):12684.

Manuscript not included in the thesis

Krstić Ristivojević M, Grundström J, Apostolović D, Radomirović M, Jovanović V, **Radoi V**, Kiewiet MBG, Vukojević V, Ćirković Veličković T, van Hage M. Alpha-Gal on the protein surface decreases transcytosis through the Caco-2 monolayer.

CONTENTS

LIST OF ABBREVIATIONS

5-HT	Serotonin, 5-hydroxytryptamine, 3-(2-Aminoethyl)-1H-indol-5-ol
5-HT_{1A}	Serotonin receptor 1A
AF	Alexa Fluor®
α-gal	Galactose-α-1,3-galactose
AP2	Adaptor protein 2
APD	Avalanche Photo Detectors
Ar/ArKr	Argon-/Krypton
B2	(8-methyl-2-{4-[4- (pyrimidin-2-yl) piperazin-1-yl] butyl}-2,8-diazaspiro [4.5] decane-1,3-dione)
B3	(8-{4-[4-(pyrimidin-2-yl) piperazin-1-yl] butyl} -8-azaspiro[4.5] decane-1,4-dione)
B5	(3-[4-[4-(4,6-dimethylpyrimidin-2-yl) piperazin-1-ium-1-yl] butyl]-5,8,8- trimethyl -3-azabicyclo[3.2.1] octane-2,4-dione;chloride;hydrochloride
BSA	Bovine serum albumin
bTG	Bovine thyroglobulin
CAMKII	Calmodulin-dependent protein kinase II
cAMP	Cyclic adenosine monophosphate
CLSM	Confocal laser scanning microscopy
CMV	Promoters for cytomegalovirus
CNS	Central nervous system
CPM	Counts per second and per molecule
CR6G	Carboxyrhodamine 6G
CREB	cAMP response element-binding protein
Cryo-EM	cryo-electron microscopy
CTxB	Cholera toxin B subunit
Cy5	Cyanine 5
CYP2D6	Cytochrome P450 Family 2 Subfamily D Member 6
DAMGO	[D-Ala2, N-MePhe4, Gly-ol]-enkephalin

DMEM	Dulbecco's Modified Eagle Medium
DRG	Dorsal root ganglia
DRt	Dorsal reticular nucleus
EDTA	Ethylenediaminetetraacetic acid
EF	Emission filter
EPR	Electron Paramagnetic Resonance
eGFP	Enhanced green fluorescent protein
ERK1/2	Extracellular signal-regulated kinase 1 and 2
FBS	Fetal bovine serum
FCS	Fluorescence correlation spectroscopy
FCCS	Fluorescence cross-correlation spectroscopy
FP	Fluorescent protein
FRET	Förster Resonance Energy Transfer
FWHM	Full width at half maximum
GABA	Gamma-aminobutyric acid
GPCR	G-protein-coupled receptor
GPI	Glycosylphosphatidylinositol
GRKs	GPCR kinases
GTP	Guanosine triphosphate
hEF-1	Human elongation factor-1
HEK 293	Human embryonic kidney 293 cells
HeNe	Helium Neon
HS	Horse serum
iMDDCs	Immature monocyte-derived dendritic cells
JNKs	c-jun N-terminal kinases
K_d	Dissociation constant
KOP	Kappa opioid receptor
LC-MS/MS	Liquid chromatography-tandem mass spectrometry
MAPK	Mitogen-activated protein kinase
MDBS	Main dichroic beam splitter
MOP	Mu opioid receptor

NA	Numerical aperture
NMR	Nuclear Magnetic Resonance
NOP	Nociceptin
NRM	Nucleus raphe magnus
NSAIDs	Nonsteroidal anti-inflammatory drugs
OIH	Opioid induced hyperalgesia
OPRM1	Opioid receptor mu 1
OVE	Observation volume element
PAG	Periaqueductal gray
PALM	PhotoActivated Localization Microscopy
PC12	Pheochromocytoma
PF14	PepFect 14
PSF	Point spread function
RCCA	Relative cross-correlation amplitude
RVM	Rostral ventromedial medulla
RPMI	Roswell Park Memorial Institute
SDBS	Secondary dichroic beam splitter
SGCs	Satellite glial cells
SIM	Structured Illumination Microscopy
siRNA	Small interfering RNA
SMLM	Single-Molecule Localization Microscopy
STAT3	Signal transducer and activator of transcription 3
STED	Stimulated Emission Depletion
STORM	Stochastic Optical Reconstruction Microscopy
tACC	Temporal autocorrelation curve
TCAs	Tricyclic antidepressants
tCCC	Temporal cross-correlation curve
τ_D	Translational diffusion time

1 INTRODUCTION

The interdisciplinary work presented in this PhD thesis addresses an important basic challenge in medicine, the pharmacotherapy of chronic pain. By examining cellular and molecular mechanisms that underlie the development of opioid induced hyperalgesia (OIH), this thesis seeks to quantitatively characterize interactions between two important receptors in order to assess their potential to serve as targets for the development of successful pharmaceutical approaches for the treatment of chronic pain.

1.1 A BRIEF OVERWIEV OF PAIN ANATOMY AND PHYSIOLOGY

1.1.1 General pathways of pain sensation

Pain, an unpleasant sensory and emotional feeling that results from physical and psychological responses to injury, is conveyed through a complex set of cellular and neurochemical interactions, *i.e.* pathways that bring together the functions of cells in specific regions in the brain, midbrain, the spinal cord and the periphery. While there are many types of pain, which differ in their underlying cellular and molecular mechanisms, as briefly discussed below, it is useful to begin by recapitulating the basics of normal pain physiology.

Briefly, under normal physiology, pain is transmitted and modulated through two principal routes, or pathways through which information flow in opposite directions. Pathways through which painful stimuli are being conveyed from the place of injury to the somatosensory cortex, part of the cerebral cortex where the information is integrated and the perception of pain is being perceived, are called nociceptive or ascending pathways. Pathways through which painful stimuli are controlled and modulated, are called anti-nociceptive or descending pathways (Fig. 1).

The very first step in pain transmission is called transduction, and refers to the process by which tissue-damaging stimuli, mechanical, chemical or thermal, activate nerve endings. For example, at the site of a peripheral injury damaged cells release various molecules. Thinly myelinated and unmyelinated sensory neurons respond to these molecules and carry the information through the peripheral branch of their axon to the dorsal root ganglion (DRG), where their somas are located, and thereafter through the central branch of their axon to the dorsal horn of the spinal cord. As the sensory neurons are the first in line to receive information about tissue injury, they are also called 1st order neurons. Within the dorsal horn of the spinal

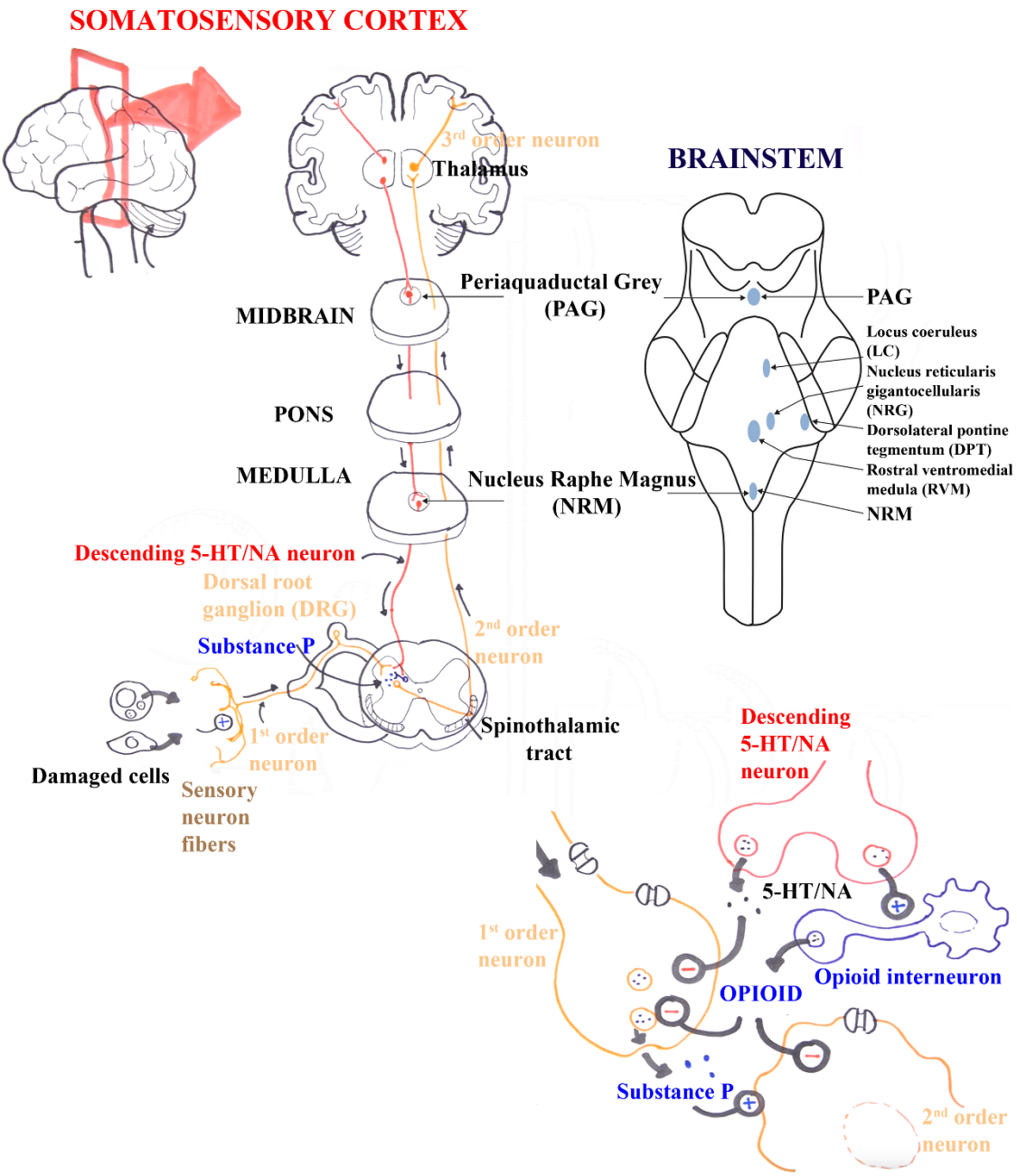

Figure 1. **Schematic drawing of the integration of pain pathways at the organism level.** Nociceptive inputs from damaged cells are transmitted through sensory neuron fibers, 1st, 2nd and 3rd order neurons comprising the ascending pathway (ocher) to the somatosensory cortex where the feeling of pain is being perceived. The descending pathways (red) originate in the somatosensory cortex, which relays to the thalamus. Thalamic neurons descend to the midbrain, where they synapse on ascending pathways in the medulla and the spinal cord and inhibit ascending nerve signals, thus soothing pain and producing pain relief (analgesia). Insert in the lower right corner shows key cells and molecules through which pain modulation is being achieved in the spinal cord, with a particular emphasis on the effective pain inhibition through the action of serotonin (5-HT) and opioid peptides. Inset in the upper right corner shows schematic drawing of the brainstem with most important functional regions depicted (see text). The image was generated using material from PAIN! Physiology - The Ascending Pathway, Descending Pain Pathway and the Substantia Gelatinosa (https://www.youtube.com/watch?v=5c8maFAhqIc), with kind permission from the Author. Inset, upper right: Image https://images.app.goo.gl/mLvBqnyoetkiofBLA, from: Lin, T. (2016). Physiology of pain. In C. Mowatt (Author) & T. Lin, T. Smith, & C. Pinnock (Eds.), Fundamentals of Anaesthesia (pp. 431-453). Cambridge: Cambridge University Press. doi:10.1017/9781139626798.023 reproduced with permission from the Publisher.

cord, the 1st order neurons form synapses and relay the signal to another set of neurons, called 2nd order neurons, by releasing substance P, an 11 amino acids long neuropeptide from the tachykinin family.

The 2nd order neurons cross over to the other side of the dorsal horn and enter a region called the spinothalamic tract (Fig. 1, ocher). From the spinothalamic tract, the 2nd order neurons ascend through the spinal cord and the brain stem, and terminate in the thalamus, with lateral projections targeting mesencephalic nuclei, including the dorsal reticular nucleus (DRt), the rostral ventromedial medulla (RVM) and the midbrain periaqueductal gray (PAG). In the thalamus, the 2nd order neurons form synapses with 3rd order neurons, which will carry on the information to a specific region in the cortex that is related with the site of injury. Thus, the 3rd order neurons help to discern the area of injury and convey the information to the relevant region of the somatosensory cortex where the information about the injury is being perceived.

The descending pathway starts in the somatosensory cortex, which relays to the thalamus and the hypothalamus (Fig. 1, red). Thalamic neurons descend to the midbrain, more precisely to the midbrain PAG. These neurons project to the nucleus raphe magnus (NRM) in the brain stem medulla, where they form synapses with serotonergic/noradrenergic neurons that secret serotonin (5-hydroxytryptamine, 5-HT) and noradrenaline (NA, also known as norepinephrine). The 5-HT/NA neurons project to the dorsal horn, more precisely to the substantia gelatinosa in the dorsal horn, where the synapses between the 1st and 2nd order neurons are located, which is also richly populated with other cell types, most notably opioid interneurons (Fig. 1, blue). Secreted 5-HT and NA suppress substance P release from the 1st order neurons and activate the opioid interneurons, which respond by secreting endogenous opioid peptides. Opioid peptides exert a dual action: (1) inhibit substance P release from the pre-synaptic 1st order neurons and (2) inhibit the depolarization of post-synaptic 2nd order neurons, thus effectively blocking the propagation of pain signal through the ascending pathway. [1-8]

1.1.2 Nociceptive and neuropathic pain

While classification of pain is not easy, as there are many aspects according to which distinctions could be made and differences between classes are not clear-cut, it is rather straightforward to distinguish two types of pain, nociceptive and neuropathic pain. Nociceptive pain is normal physiological response that results from neural pathway activation by a potential or actual tissue damage [9]. Nociceptive pain is therefore protective. Neuropathic pain is, on the other hand, caused by damage to the nervous system. It is, thus, a pathological process that

arises without a known, immediately preceding cause and with no need for outside stimuli to be involved [9,10]. Neuropathic pain reflects a dysfunctional nervous system, and therefore may arise through a variety of different mechanisms. For example, damage to inhibitory pathways or excessive stimulation of nociceptive pathways can shift the balance between non-noxious and noxious sensory input in such a way that pain arises without there being any noxious stimuli[9,11].

Furthermore, pain can be classified with respect to duration and onset.

1.1.3 Acute pain

Acute pain is a physiologically normal and healthy response to offensive stimuli. It can be directly related to a cause, is of short duration and gradually resolves as the injured tissues heal. It enables an organism to detect when normal homeostasis has been disrupted and to modify its behavior as the need dictates [7]. Thus, it is a protective, warning mechanism that communicates to the individual to withdraw from harmful stimuli [7,8]. The pain transmission mechanism succinctly described in subsection 1.1.1, outlines key steps in acute pain transmission. It is, however, important to bear in mind that qualitative and quantitative tissue-specific differences at a more detailed level of description exist [7].

Acute pain can be treated at different levels of organization of the pain transmission system. For example, pain transduction, *i.e.* conversion of the noxious stimulus to electrical signals, which is the initial step in pain transmission, can be inhibited by nonsteroidal anti-inflammatory drugs (NSAIDs, such as aspirin or ibuprofen) [12], opioids or local anesthetics (consisting of a hydrophilic tertiary amine and a lipophilic aromatic system combined by an ester or an amide linkage) [13]. Pain propagation through the peripheral nervous system *via* 1st order neurons, *i.e.* transmission, can be reduced by local anesthetics and agonists at the alpha2-adrenergic receptor (*e.g.* clonidine, tizanidine, dexmedetomidine) [14]. Modulation of interactions between 1st and 2nd order neurons in the dorsal horn cells of the spinal cord can be influenced by local anesthetics, alpha2-adrenergic receptor agonists, opioids, NSAID's, tricyclic antidepressants (TCAs) and NMDA receptor antagonists [15]. Finally, perception, *i.e.* the cerebral cortical response to nociceptive signals projected by 3rd order neurons, can be inhibited by general anesthetics, opioids and alpha2-adrenergic receptor agonists [15-17].

1.1.4 Chronic pain

Chronic pain is a serious health issue worldwide. It not only generates considerable suffering for those affected, but also generates economic burdens for both, the patient and the society [3,8], as it is among the top ten causes of disability in the world [18]. Chronic pain is defined as an unpleasant sense of discomfort that persists or recurs over long time, typically longer than 3 to 6 months. Chronic pain often presents as result to disease or injury, but is not viewed as only an accompanying symptom or an affliction, rather as separate condition [18], whereas, acute pain is viewed as a physiologically normal and healthy response [7]. When pain is persistent, pain transmitting components of the peripheral and central nervous system display great plasticity, which in turn leads to elevated pain signaling and generates hypersensitivity. This plasticity can be advantageous, as it promotes protective reflexes. It is when this persists that a chronic pain state may develop [6,19]. The reason why acute pain sometimes can transition into a chronic state has yet to be fully understood. A hypothesis gaining a lot of ground is neuroinflammation and, subsequent, glial cell activation as a key mechanism of acute pain transitioning to a chronic state [19,20]. By converting from resting state to a hyperactive state, glial cells, microglia and astrocytes exhibit a dynamic plasticity [2,19]. Mitogen-activated protein kinases (MAPKs) have been indicated as crucial mediators in intracellular cascades, during glial activation. MAPKs includes three main kinase family subtypes, namely ERKs, p38 and c-jun N-terminal kinases (JNKs) [3,16,21].

The most common treatments for nociceptive pain are opioids [13], nonsteroidal anti-inflammatory drugs (NSAIDs), paracetamol [12]. Common treatments for neuropathic pain include anticonvulsants and antidepressants [22]. Opioids are most commonly used to elevate severe pain [13]. Acute and chronic pain differ in their response to pharmacotherapy, with chronic pain often being nonresponsive to treatment with commonly used analgesics [3-8]. Despite their limited effects for treatment of chronic pain, patients with chronic pain are often prescribed analgesics, including opioids. The analgesic properties of opioids have been known for thousands of years and while their effect is well recognized for acute/subacute nociceptive pain conditions, their role in chronic pain remains controversial [23,24]. Opioids elicit side effects, which include respiratory depression, vomiting, nausea and constipation. The major concern for chronic pain patients, however, is tolerance build up, opioid induced hyperalgesia (OIH) and withdrawal [1,25].

1.2 MOLECULAR BASIS OF PAIN – FOCUS ON G PROTEIN-COUPLED RECEPTOR REPRESENTATIVES MOP AND 5-HT$_{1A}$

G protein–coupled receptors (GPCRs) constitute the largest superfamily of transmembrane receptors. Members of this family share conserved sequence motifs and the seven-pass transmembrane topology, and their function is to transmit information from the surroundings to the cellular interior [26]. Extracellular stimuli transduced by GPCRs are diverse, ranging from physical stimuli, in the form of light, heat or mechanical force, to chemical stimuli with various compounds, such as peptides/proteins, sugars, lipids. It is therefore fair to say that GPCRs mediate and/or modulate virtually all physiological processes in eukaryotic organisms, including acute and chronic pain.

GPCRs transduce external stimuli *via* two principal signaling pathways: (1) through the heterotrimeric G proteins, which was the first signal transduction pathway to be understood and to which GPCRs owe their name, or *via* (2) arrestins, initially described as proteins that turn off G protein signaling, since recruitment of arrestins, following the phosphorylation of GPCRs by GPCR kinases (GRKs), blocks GPCRs interaction with G proteins [27-31]. Traditionally, it was assumed that GPCRs exist in two distinct conformations, active and inactive, and that the active GPCR conformation is the one that is preferred by both, G proteins and GRKs/arrestins – the classical extended ternary complex model of GPCR-driven signaling. However, structural studies by X-ray crystallography and cryo-electron microscopy (cryo-EM) and advanced Nuclear Magnetic Resonance (NMR) and Electron Paramagnetic Resonance (EPR) based techniques reveal that unliganded GPCRs exist in equilibrium between multiple conformations (basal equilibrium), which specific ligands partially shift towards different conformations [27-31]. Now, while there are different active and inactive conformations, there is thus far no evidence that conformations preferred by G proteins and GRKs/arrestins are different. Thus, within the limitation of current techniques, the active GPCR conformation preferred by G proteins and GRKs/arrestins is one and the same [27-31] (Fig. 2).

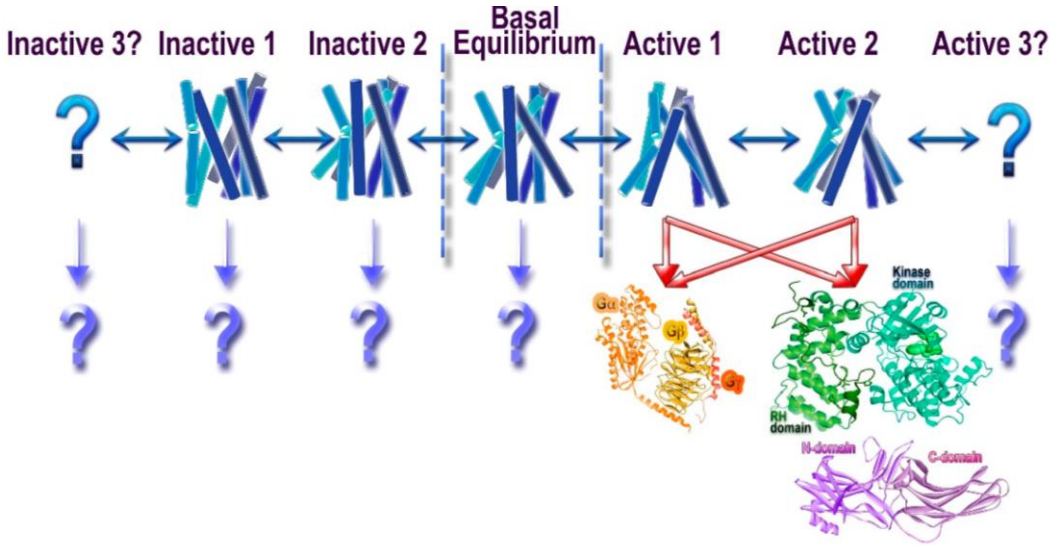

Figure 2. Conformational heterogeneity of G protein-coupled receptors (GPCRs) and signaling. In untreated cells, unliganded GPCRs appear to exist in an equilibrium between multiple conformations, so-called basal equilibrium. Agonists shift this equilibrium towards active conformations. Antagonists have no effect on their own, but block agonists' access to the receptor. The great majority of active conformations effectively couple to G proteins and GRKs/arrestins, but there are likely some that might preferentially engage distinct signal transducers (biased signaling). Image reproduced from reference 27: Gurevich and Gurevich, Int. J. Mol. Sci. 2017 **18(12):** 2519 (permitted under the Creative Commons Attribution License).

Receptor mediated signaling that arises due to spontaneous population of the active receptor conformations in the absence of a specific ligand is called constitutive activity. Agonist binding to a GPCR stabilizes the receptor in an active conformation that interacts with its cytoplasmic partner. When these partners are the heterotrimeric G proteins, ligand binding promotes the exchange of GTP for GDP from the G_α subunit. The GTP-bound G_α subunit dissociates from the $G_{\beta\gamma}$, and the GTP-liganded G_α and $G_{\beta\gamma}$ separately stimulate various effector molecules thereby activating/inhibiting the production of a number of second messengers inside the cell, including the MAPKs such as ERK1/2 and p38 [29-28]. When agonist binding facilitates the phosphorylation of the C-terminal tail by GRKs, leading to the recruitment of arrestins, downstream signaling pathways distinct from those mediated by G proteins are being activated, such as endocytosis through interactions with the clathrin adaptor protein 2 (AP2) complex, but also common ones, such as ERK1/2 signaling.

The existence of equilibrium between multiple active and inactive GPCR conformations in unstimulated cells, before they are being treated with specific ligands, is crucial for understanding the complexity underlying GPCR-ligand pharmacology. In line with this, the efficacy of a ligand is described with respect to the extent to which it can potentiate the signaling pathway that is dominant in unstimulated cells [27,30-32]. Thus, agonists promote activity above the basal level through the dominating signaling pathway, *i.e.* they favor action through the active conformation of the receptor. Endogenous ligands are *per* definition full agonists.

Partial agonists also act on the active conformation but produce weaker maximal activity at saturation than full agonists. Inverse agonists lower the activity through the dominating signaling pathway below the basal state level recorded in untreated cells by favorably acting on the inactive conformation of the GPCR. Neutral antagonists do not affect the basal activity, but compete with agonists for the same ligand-binding site. Finally, some ligands can stimulate both G protein and arrestin pathways, or multiple G proteins, and the greater efficacy toward one or the other is known as ligand bias. The ability of some ligands to stimulate both pathways may be responsible for many of the undesired effects of drugs targeted to GPCRs [30].

The equilibrium between the active and inactive conformations is dynamic and the residence time of GPCRs in the active/inactive conformations is, while receptor- and ligand-specific, in the sub-millisecond to tens of milliseconds range [27-31]. In addition, it is important to note that even at full signaling, only a portion of the receptors are occupied by the ligand. Thus, only a fraction of receptors are activated during a full signaling response, while the remaining receptors comprise the so-called receptor reserve [33].

While numerous GPCRs are implicated in pain physiology, members of the opioid and the serotonin GPCR families are the ones that are of utmost relevance for pain pharmacotherapy.

1.2.1 Opioids and opioid receptors

The endogenous opioid system consists of four opioid receptor types: mu- (MOP), kappa- (KOP), delta- (DOP) and nociceptin (NOP), and their corresponding endogenous peptide ligands: endorphins, dynorphins, enkephalins and nociceptin/orphanin FQ, respectively. Opioid receptors and opioid peptides are widely expressed across the nervous system, and pain pathways in particular. They modulate the nervous system function at all levels of integration, including autonomic, sensory, emotional and cognitive processing. MOP, DOP and KOP facilitate spinal analgesia, with MOP also mediating supraspinal analgesia [34].

At the cellular level, opioid receptors activate G protein dependent and independent signaling pathways. G protein dependent pathways involve both, signaling through the inhibitory G_i/G_o subtypes of G_α and the $G_{\beta\gamma}$ subunits, leading to the inhibition of cAMP, opening of K^+ and closing of Ca^{2+} channels. G protein-independent signaling cascades include arrestin-mediated activation of ERK1/2 and c-Jun N-Terminal Kinase 2. Moreover, activation of the p38 MAPK, protein kinases A and C, signal transducer and activator of transcription 3 (STAT3) and,

calmodulin-dependent protein kinase II (CAMKII) were also observed, but whether these pathways are dominantly activated *via* G proteins or arrestins is not clear [35-38].

While all opioid receptors are implicated in the modulation of pain, deletion of the *OPRM1* gene has shown that MOP alone is responsible for both, the therapeutic and the adverse effects of morphine [39]. MOP is also the target for other clinically useful opioids, such as fentanyl, codeine and oxycodone, which were studied here. We therefore focus on MOP only.

As for other opioid receptors, intracellular effects of MOP activation are ligand-specific and include inhibition of adenylyl cyclase activity, closing of voltage gated Ca^{2+} channels, activation of inwardly rectifying K^+ channels and stimulation of MAPK pathways [40,41]. Post activation, MOPs are endocytosed and recycled back to the plasma membrane, through a pathway that includes phosphorylation by GPCR kinase and binding of arrestins. MOP endocytosis plays a key role in the occurrence of problematic side effects, from opioid treatment [41]. A recent study, in mice, showed that analgesic tolerance and OIH, caused by opioid agonists, could be limited by co-treatment with MOP antagonist [42], while another study, in rats, showed that MOP antagonists restore the antinociceptive effects of morphine by suppressing the p38 MAPK signaling pathway [43]. Additionally, chronic treatment with MOP antagonists was found to upregulate MOP in rats, but showed no increase in MOP mRNA levels, which suggested that MOP antagonists altered receptor compartmentalization, post translational modifications or turnover [36,44]

Opioids are among the most effective analgesics and play a key role in the descending anti-nociceptive pathway [1]. Exogenous opioids mimic endogenous opioid peptides in PAG, RVM and the spinal dorsal horn to induce analgesia [4]. Immune cells synthesize and secrete endogenous opioid peptides like β-endorphin, Met-enkephalin and dynorphin, in response to stress stimuli causing secretion of the corticotropin-releasing factor or hormone [10].

New tools and innovative approaches are revealing that opioid receptors are more complex than previously appreciated [13,45,46]. They bring new insights into how opioid receptors signal and reveal the significance of receptor trafficking [47-49]. For example, Erbs et al. showed in knock-in mice that interactions between MOP and DOP could be either at system-level or heteromerization, depending on the region of the brain [47].

1.2.2 Serotonin and Serotonin receptors

In mammals, 5-HT works as a neurotransmitter in the central and peripheral nervous system. The RVM includes, among other structures, the serotonin-rich NRM [4]. 5-HT is associated with a multitude of physiological and pathological processes, including functioning as a local hormone in some tissues. The serotonin receptor 1A (5-HT_{1A}) is part of the 5-HT_1 family, which also includes 5-HT_{1B}, 5-HT_{1D}, 5-HT_{1E} and 5-HT_{1F}. Like the opioid receptors, this receptor family couples to $G_{i/o}$, which inhibit adenylyl cyclase and lowers cAMP levels. Activation of 5-HT_{1A} also activates the ERK1/2 MAPK signaling pathway, although this is believed not to be a universal response in the brain [50]. 5-HT_{1A} has a wide distribution in the CNS [51,52]. It is also found in dendrites, the soma and sometimes in the axon hillock of neurons. All serotonin neurons express 5-HT_{1A}, as do many nonserotonergic neurons. Activation of 5-HT_{1A} has a general inhibitory electrophysiological effect, manifested in reduced neuronal firing rates. Several neuropsychiatric disorders are thought to have a 5-HT_{1A} pathway which, consequently, has made 5-HT_{1A} a therapeutic target. Clinically used ligands include partial agonists, neutral antagonists [12] and full agonists (the drug buspirone acts as a full agonist on presynaptic 5-HT_{1A} and as a partial agonist on postsynaptic 5-HT_{1A}) [53,54]. Buspirone was first introduced as an anxiolytic in 1986 [55,56]. It belongs to the class of drugs referred to as azapirones, of which there are currently two approved drugs (buspirone and tandospirone) [57]. Since its introduction, studies on buspirone have included combinatory/augmentation strategies for depression, immune system modulation in HIV, ethanol consumption and morphine tolerance, to name but a few [58-61]. Augmentation of morphine treatment with buspirone was found to elicit a better pain control response and helped to hamper the development of tolerance in animals [61].

1.2.3 MOP and 5-HT_{1A} receptor interactions

GPCR homo- and heterodimerization is an important mechanism through which cellular signaling repertoire can be expanded without the need for designing new biological molecules. Many GPCRs form functional homo- and heterodimers, and so does MOP, as documented in numerous studies recently reviewed by Massotte [62]. However, heterodimer formation between MOP and 5-HT_{1A} was thus far documented in one study only [41], even though numerous studies reveal the co-expression and co-localization of MOP and the 5-HT_{1A} in discrete areas of the brain, such as PAG neurons, dorsal raphe nucleus, dorsal horn of the spinal cord, amygdala and primary afferent nociceptive fibers, suggesting that these receptors function in close adjacency to one and other. Although the interactions between opioid and serotonergic signaling are not

fully understood [1,63], the cAMP pathway is known to crosstalk with the MAPK pathway, with key interactions involving ERK1/2 and p38 [64]. Furthermore, genetic studies indicate an interaction between 5-HT_{1A} and MOP signaling on the function of endogenous descending pain inhibition in healthy subjects and pain patients [65] as well as an effect of serotonergic signaling on opioid induced analgesia in healthy subjects [66]. The 5-HT_{1A} receptor is an inhibitory presynaptic autoreceptor on serotonergic neurons and is also expressed postsynaptically in terminal regions innervated by serotonergic neurons [67]. The 5-HT_{1A} and MOP receptors co-localize on individual presynaptic GABAergic nerve terminals and have been demonstrated to synergistically inhibit GABA release in PAG, thus likely affecting analgesia [41]. Through behavioral studies, on morphine addiction and tolerance, a hypothesis of cooperation between MOP and 5-HT_{1A} has been suggested [41]. In animal studies, 5-HT_{1A} receptor agonists have been reported to counteract opioid-induced hyperalgesia, opioid tolerance and to improve the analgesic potential of opioids while reducing their rewarding effects [63,68,69]. This strategy is believed to engage serotonergic input from the raphe nuclei to the ventrolateral PAG. Serotonin, in addition, also regulates the opioid-induced descending antinociceptive pathway [41]. Contrary to opioids, a first order pronociceptive effect followed by a second order analgesic effect has been documented for 5-HT_{1A} agonists, suggesting opposing effects between opioids and 5-HT_{1A} agonists [68]. Therefore, hypothetically, 5-HT_{1A}/MOP interactions could be time-dependent with 5-HT_{1A} antagonists initially enhancing opioid analgesia [70,71] while 5-HT_{1A} agonists would have beneficial long-term effects, when OIH has presented [63,68,69]. In clinical settings, serotonin selective reuptake inhibitors (SSRIs) have not been found to have an analgesic effect on patients. However, analgesic effects have been shown by tricyclic antidepressants and serotonin- and noradrenalin reuptake inhibitors (SNRI) [72]. In addition, MOP have been shown to modulate the effects of 5-HT_{1A} agonists in rats [73]. Furthermore, a study of HEK 293 cells demonstrated formation of functional MOP/5-HT_{1A} heterodimers and that signaling of one receptor in the MOP/5-HT_{1A} heterodimer was inhibited by activation of the other receptor, i.e., pretreatment with a 5-HT_{1A} agonist abolished subsequent ERK1/2 activation by a MOP agonist [41].

2 AIM

Based on inferences made from clinical studies by Kosek et al. [66], it was hypothesized that heterodimer formation between MOP and 5-HT_{1A} receptors may underlie the development of OIH. The primary aim of my work was to challenge the hypothesis that prolonged exposure to non-peptide opioids promotes heterodimer formation between MOP and 5-HT_{1A} receptors, and that this effect can be abolished by co-treatment with 5-HT_{1A} agonists. To this overall aim:

- The first objective of my work was to use molecular cloning to develop cell lines of human and rat origin that stably express physiologically relevant levels of MOP and 5-HT_{1A} receptors tagged with spectrally distinct fluorescence reporters.
- The second objective of my work was to use advanced fluorescence microscopy imaging and correlation spectroscopy techniques to quantitatively characterize in live cells interactions between MOP and 5-HT_{1A} receptors and to characterize the consequences of agonist exposure on intracellular signaling.
- The third objective of my work was to characterize the effect of selected non-peptide opioids on the extent of MOP and 5-HT_{1A} heterodimerization.
- The fourth objective of my work was to investigate wether non-peptide opioid-induced MOP and 5-HT_{1A} heterodimerization can be abolished by co-treatment with 5-HT_{1A} agonists.

In **Paper I**, we showed that prolonged exposure to non-peptide opioids facilitated heterodimer formation between MOP and 5-HT_{1A} receptors in live cells expressing physiologically relevant receptor levels. The extent of receptor heterodimerization was found to be both, opioid-specific and dose-dependent. Furthermore, we showed that different opioids differently affected second messenger pathways, as indicated by differences in Ca^{2+} signaling dynamics and differential activation of p38 and ERK1/2 pathways.

In **Paper II**, we showed that 5-HT_{1A} agonists such as buspirone and three newly identified buspirone analogs: B2, B3 and B5, can effectively reverse MOP–5-HT_{1A} heterodimerization, thus counteracting the aversive effects of morphine. Importantly, this study, which brought together molecular modeling, virtual screening and advanced experimental tests in live cells, may in the future lead to the development of new drugs that target MOP and 5-HT_{1A} heterodimer formation.

In **paper III**, we have quantitatively characterized using FCS/FCCS and PhotoActivated Localization Microscopy (PALM) the nanoscale lateral dynamics and spatial organization of wild type MOP and its naturally occurring isoform MOP_{N40D}, and showed that these properties

important determinants of opioid receptors' function. In particular, we found MOP to be largely excluded from GM1 ganglioside-enriched domains and associate with cholesterol and GPI-enriched domains. We demonstrated that these properties can be altered under the influence of exogenous substances, such as drugs, but may also be altered in disease conditions, leading to altered kinetics of ligand-receptor interactions and the receptor-mediated signaling dynamics. We also showed that MOP and MOP_{N40D} differ with respect to nanoscale lateral dynamics and organization, which may, at least in part, explain why carriers of the MOP_{N40D} isoform differ with respect to their response to pain, analgesics and substances of abuse.

In addition, an important objective of my PhD training, was to implement advanced fluorescence microscopy and correlation spectroscopy-based analytical techniques for the study of molecular mechanisms that underlie cellular uptake. Papers IV and V describe collaborative work where CLSM and/or FCS/FCCS were used to characterize translocation across the plasma membrane and cellular uptake of biomolecules.

In **Paper IV**, FCS/FCCS was used to reveal the heterogeneity underlying self-assembly of cell-penetrating peptides and oligonucleotides, in this case small interfering RNA (siRNA), into large molecular complexes. We showed that peptide monomers, peptide self-aggregates and polydisperse peptide/cargo complexes coexist in solution and in live cell plasma membrane, which could at least in part explain why diverse cellular uptake mechanisms were simultaneously observed for cell-penetrating peptides-based delivery of cargo molecules.

In **Paper V**, cellular and molecular mechanisms underlying the development of allergy to red meat were investigated, with a particular focus on the role of α-Gal carbohydrate on protein uptake and degradation by immature monocyte-derived dendritic cells (iMDDCs). CLSM imaging revealed that presence of allergenic α-Gal epitopes on the protein surface significantly increases the uptake of the investigated model antigens, BSA-α-Gal and HSA-α-Gal, by *in vitro* cultured human iMDDCs, and showed that the taken up proteins are processed in endosomes.

3 RESEARCH APPROACH

The main technique utilized in this thesis to quantitatively characterize the interactions between MOP and 5-HT_{1A} receptors is Fluorescence Cross-Correlation Spectroscopy (FCCS). FCCS is a non-destructive, highly sensitive and inherently quantitative technique that is well suited for studies of molecular interactions in live cells because it can identify bound molecules as they move together and quantitatively characterizes their concentration without having to separate the free and bound fractions [55]. FCCS is more versatile and better suited for such studies than the Förster Resonance Energy Transfer (FRET) assay that is commonly used [74]. While for efficient non-radiative energy transfer to occur the molecules need to be very close to one another, at distances shorter than 10 nm, the fact that two molecules are in the vicinity of one another does not necessarily mean that they interact. Thus, FRET is a proximity assay, rather than a true binding assay. Moreover, FRET efficiency is hampered by false negative results due to steric hindrances – for resonance energy transfer to occur, efficient dipole–dipole coupling between the fluorophores that constitute the donor-acceptor pair needs to be achieved. This, in turn, means that resonance energy transfer will only take place in a small population of properly oriented molecules. Such requirement does not exist in FCCS.

In addition to FCCS, complementary fluorescence techniques as well as classical biochemical assays were utilized to thoroughly explore the consequences of the molecular interactions and cellular responses described in the introduction. The research approach section includes an introduction to FCCS, fluorescence correlation spectroscopy (FCS) as well as confocal laser scanning microscopy (CLSM). The author also presents selected protocols applied throughout the five research papers and statistical analysis. Additional methods and methods contributed by co-authors are described in detail in the research papers included in this thesis.

3.1 THEORY OF FCS AND FCCS

Since its inception, almost 50 years ago, Fluorescence Correlation Spectroscopy (FCS) has developed from an abstruse measurement technique to a widely utilized research tool that is of particular value for nondestructive quantitative analysis in live biological specimen [75]. This quantitative technique with high temporal (sub-microsecond) and spatial (sub-micrometer) resolution and the ultimate, single-molecule sensitivity, relies on the analysis of fluorescence intensity fluctuations around an average value (equilibrium or non-equilibrium stationary state) to extract quantitative information about the concentration and diffusion of fluorescent molecules, when the fluorescence intensity fluctuations are generated by molecular diffusion,

and/or the kinetics of a blinking process, when the fluctuations are generated by molecules alternating between dark and bright states [76,77]. FCS acquired its ultimate sensitivity and real-time analysis feature when it was realized that the arrangement of optical elements that is employed in confocal microscopes can be utilized to generate a minute observation volume element (OVE) in the sample. The volume is nowadays typically 0.1 – 2 fl ($0.1 – 2\times10^{-15}$ l). This reduction in OVE size that was achieved by integrating FCS with confocal microscopy, significantly decreased the background from surrounding molecules, markedly improving the signal-to-noise ratio and, thus, FCS sensitivity [26,75,76].

Fluctuations in fluorescence intensity are typically evaluated using temporal autocorrelation analyzis. For nonrandom fluctuations, temporal autocorrelation analysis of the fluorescence intensity fluctuations generates a decaying temporal autocorrelation curve (tACC), where the amplitude at the zero-lag time is inversely proportional to the average number of molecules in the OVE and the characteristic decay time contains information about the diffusion of molecules [78-80] [75,78,80-84]. Briefly, a time-dependent fluctuation in fluorescence intensity is expressed as a fluorescence signal at time *t*, F(t), measured against the time-averaged signal ⟨F(t)⟩ [78,80].

$$\delta F(t) = F(t) - \langle F(t) \rangle \quad (1)$$

and the normalized autocorrelation curve is calculated as:

$$G(\tau) = 1 + \frac{(\delta F(t)\delta F(t+\tau))}{\langle F(t) \rangle^2}, \quad (2)$$

where the fluorescence intensity fluctuation trace is compared to a "shifted" version of itself. The "shift", called the lag time, τ, is varied to identify whether there is a characteristic value of τ after which the correlation is being lost [76,80].

The average time a fluorescent molecule resides in the OVE, the so-called residence time, or the average time that it takes a molecule to "cross" the OVE by translational diffusion, called the translational diffusion time, is designated τ_D. τ_D is directly related to the size of the OVE and the diffusion coefficient (D) of the molecule:

$$\tau_D = \frac{w_{xy}^2}{4D}, \quad (3)$$

where ω_{xy}^2 is the radial radius of the OVE squared.

Molecular diffusion at the plasma membrane is two-dimensional (2D), and is often called lateral diffusion. To extract from the tACC quantitative information about the average number

of molecules in the OVE (N) and the lateral diffusion time (τ_D), the experimentally determined tACC is fitted with a theoretically derived equation for 2D-diffusion [76]:

$$G_{diff}(\tau) = \frac{1}{N}\left(1 + \frac{\tau}{\tau_D}\right)^{-1} . \quad (4)$$

The study of interactions between molecules of similar size can be problematic in FCS, as a two-fold change in size will result in a change in diffusion time that is proportional to the cubic root of two. A more suitable technique for characterizing interactions between molecules of similar size is Fluorescence Cross-Correlation Spectroscopy (FCCS) [80,85]. In FCCS, fluorescence intensity fluctuations from two spectrally distinct fluorophores are collected and analyzed, both in regards to their self-similarity (autocorrelation) and interaction (cross-correlation). Cross-correlation is a "measure" of the number of fluorescence intensity fluctuations detected simultaneously in two channels, which corresponds to two spectrally distinct molecules that are co-diffusing [78]. This analysis generates two tACCs and one temporal cross-correlation curve (tCCC).

For biological applications, fluorescent proteins which emit fluorescence in the green and red part of the spectrum are a common pair. We will therefore generally denote them as r (red) and g (green). In FCCS, the two tACC reflect the total number of green and red labeled molecules respectively, and $N_g^{total} = N_g + N_{gr}$ and $N_r^{total} = N_r + N_{gr}$. Assuming ideal conditions, (same effective volume element and fully separated absorption/emission spectra) the cross-correlation function can be described as [80,86]:

$$G_{CC}(\tau) = 1 + \frac{\langle \delta F_{green}(t) \cdot \delta F_{red}(t+\tau) \rangle}{\langle F_{green}(t) \rangle \langle F_{red}(t) \rangle} \quad (5)$$

The zero-lag time amplitude of the tCCC is directly proportional to the number of dually labeled co-diffusing molecules. Which means that as N_{gr} increases so does the amplitude of the tCCC:

$$G_{CC}(0) - 1 \propto \frac{N_{gr}}{(N_g + N_{gr}) \cdot (N_r + N_{gr})} \quad (6)$$

In order to calculate the contribution of dually labeled fluorescent molecules, the values at zero-lag time for both tACCs and the tCCC can be determined, and post-processed mathematically to generate a dimensionless value known as the relative cross-correlation amplitude (RCCA):

$$RCCA = \frac{G_{cc}(\tau) - 1}{G_{AC}(\tau) - 1} = \frac{N_{gr}}{N_r^{total}} = \frac{N_{gr}}{N_r + N_{gr}} \quad (7)$$

This analysis gives the number of double-labeled, *i.e.* heterodimer receptor complexes (N_{gr}) relative to the total number of the red labeled (N_r^{total}), including the single-labeled (N_r) and the double-labeled (N_{gr}) ones [26,85].

Strictly speaking, equations (6) and (7) are valid under the assumptions that fluorophore brightness is not changing upon binding and that there is no spectral cross-talk between the channels. The contribution due to spectral cross-talk can be corrected following procedures described in [23], [90] and [87]. Briefly, the cross-talk-induced cross-correlation needs to be subtracted from the relative cross-correlation and the remaining cross-correlation scaled up as follows:

$$RCCA_{corrected} = \frac{\mathrm{RCCA} - \kappa \cdot f}{1 - \kappa \cdot f}, \qquad (8)$$

where κ is the bleed-through ratio, *i.e.* brightness as reflected by the counts per second and per molecule (CPM) of the green dye in the red channel when the red fluorophore is not present, divided by its brightness in the green channel. For the optical setting used in our studies, κ = 0.1, and *f* is the count rate ratio in the green and red channels, $f = CR_g/CR_r \leq 0.5$. Following treatment, increase in eGFP brightness was observed, while Tomato brightness remained largely unchanged. To account for this, the κ factor was accordingly scaled, becoming, at most κ = 0.2, and the product $\kappa.f \leq 0.15$.

3.2 CONFOCAL LASER SCANNING MICROSCOPY

A confocal laser scanning microscope utilizes a specific arrangement of optical elements and spatial filtering of the fluorescence signal by pinholes to improve the signal-to-background ratio by excluding out-of-focus light [88]. CLSM utilizes point-by-point illumination of the sample and fluorescence detection. This has the drawback that few emitted photons reach the detector. This requires the sample to be illuminated for a longer time, so that each point gets sufficiently illuminated thus avoiding noisy images [88,89].

Spatial resolution of a CLSM system depends on the numerical aperture (NA) of the objective lens, a dimensionless value that characterizes the light-gathering ability of the lens according to the formula:

$$\mathrm{NA} = n \cdot sin\theta \ , \qquad (9)$$

where *n* is the index of refraction of the medium in which the lens is working (n_{air} = 1.00, n_{water} = 1.33 and n_{oil} = 1.52 (for typically used immersion oils)) and θ is the maximal half-angle of the cone of light that can enter or exit the lens.

The numerical aperture and the wavelength of incident light (λ), are the main determinants of the size of the Airy pattern, a bright circular region in the center, known as the Airy disk, surrounded by concentric bright and dark rings that are formed by constructive and destructive interference, respectively, of diffracted light after passing through a lens with a circular aperture). The center of the Airy pattern (out to the first minimum) is referred to as the Airy disk and contains approximately 86 % of the total light. The Rayleigh criterion stipulates that the minimum distance between two Airy disks, for which they are distinguishable, is equal to their radii [89]. From the Airy pattern a point spread function (PSF) can be calculated. The full width at half maximum (FWHM) of the PSF gives an indication of the optical resolution of the microscope (Fig. 3).

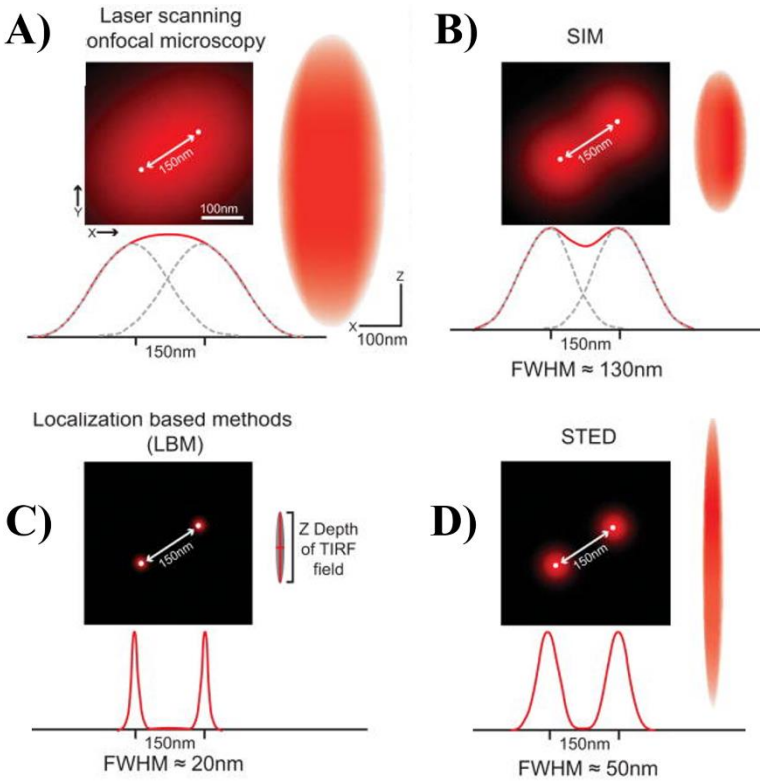

Figure 3. Appearance of two point sources separated by 150 nm *via* current commercially available diffraction-limited and super-resolution microscopes. A) Overlapping PSFs (approximated by Gaussians) typical of Confocal Laser Scanning Microscopy (CLSM). **B)** Structured Illumination Microscopy (SIM). **C)** Single Molecule Localization Microscopy (SMLM). **D)** Stimulated Emission Depletion (STED). The PSF cartoons to the right represent the effective precision associated with each method. Image reproduced from reference XX: Brian R Long, Danielle C Robinson and Haining Zhong. Subdiffractive microscopy: techniques, applications, and challenges. Wiley Interdiscip Rev Syst Biol Med. 2014 **6(2):** 151–168, with permission from the Publisher.

In the focal plane, radial direction (x and y plane), the spatial resolution limit is:

$$d_{xy} = PSF_{FWHM} \approx 0.61\lambda_0/NA \quad (10)$$

and in the axial direction (z-axis):

$$d_z \approx n\lambda_0/NA^2 \quad (11)$$

where λ_0 is the excitation wavelength and *n* the refractive index of the medium. High NA objectives can generate PSF_{FWHM} that is about 200-250 nm wide radially in the focal plane and 500-700 nm in the optical axis. Although noteworthy, this resolution cannot confidently resolve structures that are smaller/objects that are closer than 200 nm, which remains a challenge for many applications in life sciences (Fig. 3A) [13]. The limitation in spatial resolution due to diffraction of light, which is known as the diffraction limited spatial resolution, is circumvented in super-resolution fluorescence microscopy techniques [90,91]. There are three principally different ways how this can be achieved. Briefly, in Structured Illumination Microscopy (SIM)[92,93], a high NA objective (NA = 1.7) and a movable diffraction grating placed in the path of the laser beam are used to illuminate the sample in a stripe pattern generated by interference, for which the minimum stripe distance is close to the resolution limit. To achieve high spatial resolution in all directions, a series of raw images is consecutively acquired with translationally phase-shifted and rotated illumination. The information is then retrieved through mathematical reconstruction and a contrast-enhanced image with a two-fold increased lateral and axial resolution is obtained (Fig. 3B). However, due to errors in grating position, system calibration, refractive index mismatch, sample heterogeneity and poor quality artifacts in a SIM image can be introduced that are difficult to recognize and remove. Also, SIM is slow, requiring 1 – 30 s processing time, which may be too slow for the study of fast processes.

Like SIM, Single-Molecule Localization Microscopy (SMLM) is a wide field imaging technique that includes methods such as PhotoActivated Localization Microscopy (PALM) and Stochastic Optical Reconstruction Microscopy (STORM). In SMLM, a small subsets of individual molecules are randomly activated or switched on/off in consecutive acquisitions. If sparse enough, single-molecule switching events are identified. By collecting the signal over several thousands of camera frames, the signals become spatiotemporally separated. Raw data are thereafter processed to detect single molecules and determine their centers of positions. The precision with which the centers of position of an individual molecule can be determined depends on the number of photons detected *per* individual molecule. In SMLM, the standard

error of the mean of the PSF, which is a measure of the localization precision, can be made arbitrarily small by collecting more photons and by minimizing the noise factors [94,95]:

$$\sigma = \sqrt{\frac{s^2}{N} + \frac{a^2}{12N} + \frac{8\pi s^4 b^2}{a^2 N^2}}\ , \qquad (12)$$

where *s* is the standard deviation of the Gaussian distribution that equals 1/2.2 of the PSF width, *a* is the pixel size, *b* is the background and *N* is the number of collected photons. Thus, by collecting a sufficient number of photons, *N* = 10 000, the errors due to: the photon noise (first term in eq. (12)), finite pixel size of the detector (second term in eq. (12)), error due to the effect of the background (third term in eq. (12)), all become very small and individual molecules can be localized with a nm precision. Finally, all localizations of individual molecules with their corresponding localization precision are then assembled through superimposition into a single-plane super-resolution SMLM image (Fig. 3C). Like SIM, SMLM is slow and requires computational post-processing. It therefore cannot be easily used to study fast dynamic processes. An additional limitation originates from the high number of emitted photons that are required to achieve a sufficient signal-to-noise ratio. The number of photons that need to be collected is proportional to the number of pixels in the image, and increases in proportion to the square (for 2D) or the cube (for 3D) imaging.

In STED microscopy [96], a depletion laser beam with a local intensity minimum in the center is superimposed on the confocal excitation beam. The depletion laser forces molecules excited by the confocal excitation laser to undergo stimulated, rather than spontaneous de-excitation, thus effectively preventing fluorescence emission from other locations than the local intensity minimum. Efficient restriction of spontaneous fluorescence emission to the central region enables imaging of sub-diffraction scales (Fig. 3D). Unlike SIM and SMLM, which are wide-field techniques, STED is a scanning technique, which means that there is a time delay across the image. On the positive side, this means that computational post-processing is not necessary, although deconvolution is often applied to compensate for low signal in samples with increased background. Like SMLM and SIM, STED is not well suited for the study of fast dynamical processes. Also, STED is not quantitative, if not coupled with FCS [97]. Finally, the most serious limitation of STED microscopy for applications in biomedical research is high photobleaching and high photo-toxicity.

3.3 CELL MODEL

The most common strategy for live cell fluorescence experiments is to genetically modify cells to stably express recombinant proteins, *i.e.* proteins of interest coupled to fluorescent proteins[98,99]. This strategy can be applied to commercially available immortalized mammalian cell lines [100]. One of the most commonly used mammalian cell line for expressing recombinant proteins is the human embryonic kidney cell line (HEK 293) [100,101]. Despite having an epithelial origin, HEK 293 cells are capable of most post translational folding and modifications required to produce mammalian proteins. HEK 293 cells are viewed as a good system when evaluating pharmacological properties [101]. The rat phaeochromocytoma (PC12) cell line is a popular mammalian cell line owing to its versatility for pharmacological manipulation [102].

Both HEK 293 and PC12 cells can be transfected to stably express recombinant proteins via the method of lipofection [101,103,104]. By using a mammalian dual expression vector (pBudCE4.1), with two strong promoters (CMV and hEF-1) [100], both HEK 293 and PC12 cells can be transfected to express MOP and 5-HT_{1A}, coupled to spectrally distinct fluorescence proteins. Conventionally green and red shifted fluorescent proteins (FP) are used. Among the red shifted FP a common family is the "mFruit" family (m stands for monomeric). This class of FP showcase a wide range of red shifted colors, however, most mFruit FP suffer from low intrinsic brightness and poor photostability. The dimeric red shifted FP Tomato, is a derivative of the mFruits, that has better brightness and photostability than its monomeric counterparts [84].

3.4 PROTOCOLS

3.4.1 Cell culturing

Both HEK 293 and PC12 cells were cultured in collagen-coated T25 flasks (SARSTEDT). HEK 293 cells where grown in DMEM medium supplemented with 10 % fetal bovine serum (FBS) and PC12 cells in RPMI 1640 medium supplemented with 10 horse serum (HS) and 5 % FBS. Both growth media were supplemented with 100 U / mL penicillin and 100 µg / mL streptomycin (PenStrep) (all from Invitrogen, Sweden). Both cell lines were cultured at 37°C in a humidified 5 % CO_2 incubator.

3.4.2 Cell transfection

Both HEK 293 and PC12 cells were seeded in eight-well Nunc™ Lab-Tek™ Chambered Coverglass with 1.0 borosilicate bottom (Thermo Scientific) to a total volume of 300 µl per well. Cells were transfected with Lipofectamine 2000 (Invitrogen, Sweden), using the manufacturer's transfection protocol (for an eight-well system: 400 ng of DNA and 2.5 µl of

Lipofectamine 2000). For both cell lines the growth medium was changed to Opti-MEM (Invitrogen, Sweden) during the transfection.

For dual expression experiments the cells were transfected with pBudCE4.1 plasmid, which can express two genes simultaneously via CMV and hEF-1 promoters. MOP fused with enhanced green fluorescent protein (eGFP) is expressed under control of hEF-1 promotor (KpnXho) and 5-HT_{1A} fused with the red fluorescent protein dimeric tomato red (Tomato), under control of CMV promoter (HindXba) [100]. Stably expressing cells (Fig. 4) were isolated through selection with phleomycin D1 antibiotic (0.4 mg/ml, ThermoFisher).

3.4.3 CLSM imaging

The CLSM/FCCS measurements were carried out on an in-house ConfoCor3 (Carl Zeiss, Jena, Germany), with unique modifications. The system comprises an inverted microscope for transmitted and epifluorescent (Axiovert 200 M) light; a VIS-laser module housing an Ar/ArKr laser (458, 477, 488 and 514 nm), a HeNe (543 nm) laser and a HeNe (633 nm) laser; scanning module LSM 510 META modified to enable imaging with silicon avalanche photodiodes (SPCM-AQR-1X, PerkinElmer, USA) and a FCS module with three detection channels (Figure 1A). In all experiments with live cells a C-Apochromat 40× /1.2 W UV-VIS-IR objective (Zeiss MicroImaging GmbH, Jena, Germany) was used (**papers I-IV**). For imaging of fixed samples an alpha Plan-Fluar 100×/1.45 oil immersion objective (Zeiss MicroImaging GmbH, Jena, Germany) was used (**paper V**).

CLSM images were acquired in a sequential, *i.e.*, dual track mode, one channel at a time. eGFP fluorescence was excited using the 488 nm line of the Ar/ArKr laser. A band pass 505-530 nm emission filter was used to spectrally narrow the emitted fluorescence. Tomato fluorescence was excited using the 543 nm HeNe laser, and a long pass 580 nm emission filter was used to collect the emitted fluorescence. Incident and emitted light were separated using the main dichroic beam splitter HFT 488/543/633. eGFP and Tomato fluorescence were separated using a secondary dichroic beam splitter NFT 545 (Fig. 4A). Images were acquired without averaging, using a pixel dwell time of 51.2 µs and a 512×512 pixels format (Fig. 4B).

For live cell imaging an incubation stage was used, consisting of heated microscope stage (Heating insert P), incubator box (Incubator S), atmosphere-controller (CTI-Controller 3700, supplying cells with heated mixture of CO_2 and air) fitted with a humidifier and a temperature regulator (Temp control 37-2 digital). The temperature and CO_2 levels were continuously monitored and regulated via a digital feedback control algorithm, allowing for optimal control of all parameters.

3.4.4 FCS / FCCS measurements on the plasma membrane

For experiments on the plasma membrane, an axial *z*-scan was first performed, with a step length of 0.5 µm (**papers I-IV**). The scan generates a graph with two distinct peaks, which reveal the position of the basal and the apical plasma membrane (Fig. 4C). Fluorescence intensity fluctuations were recorded in arrays of 10 consecutive 10 s measurements when a single wavelength was used (FCS), and 20 s measurements when two wavelengths were used (FCCS) (Fig. 4D). The same optical setup was used for FCS/FCCS as for CLSM imaging.

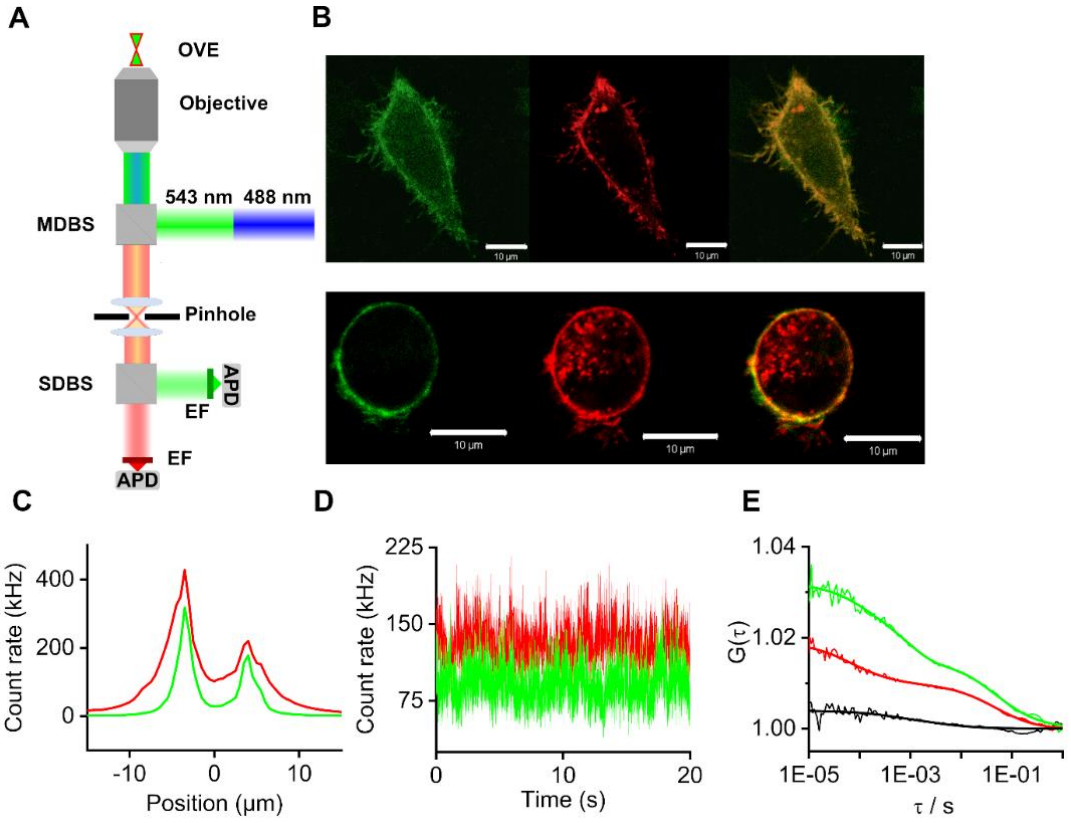

Figure 4. FCCS measurement in live cells. A) Schematic representation of the optical setup in an inverted epifluorescence confocal microscope for dual color imaging and FCCS. Incident light from two lasers, 488 nm (blue) and 543 nm (green) are merged and reflected by the main dichroic beam splitter (MDBS) and focused sharply onto sample. Both incident (blue and green) and the spectrally distinct fluorescent light (green and red) scatter elastically and are collected by the objective and separated by the MDBS. The emitted fluorescent light is further spectrally narrowed using a secondary dichroic beam splitter (SDBS) and matching emission filters (EF), before being recorded by Avalanche Photo Detectors (APD) detectors. **B)** CLSM images of HEK 293 (above) and PC12 (bellow) cells stably transformed to express MOP-eGFP (green) and 5-HT_{1A}-Tomato (red). Scale bar 10 µm. **C)** Fluorescence intensity scan the axial direction through a HEK 293 cell expressing MOP-eGFP (green) and 5-HT1A-Tomato (red). The scan has two distinct peaks corresponding to the basal (firs) and apical (second) plasma membrane. **D)** Fluorescence intensity fluctuations recorded at the apical plasma membrane of a HEK 293 cell stably transformed to express MOP-eGFP (green) and 5-HT_{1A}-Tomato (red). **E)** Corresponding temporal autocorrelation curves (green and red) and the cross-correlation curve (black) from D. The cross-correlation curve corresponds to the simultaneous passage of MOP-eGFP and 5-HT_{1A}-Tomato through the OVE.

The fluctuations in fluorescence intensity were analyzed using temporal autocorrelation analysis, yielding two distinct temporal autocorrelation curves (tACC), one for each monomeric species (Fig. 4E, green and red) and one temporal cross-correlation curve (tCCC) for the dimeric species (black) (Fig. 4E). Contrary to the amplitude of the tACC, which is

inversely proportional to the average number of molecules (*N*) in the OVE (eq. (4)), the cross-correlation curve amplitude is directly proportional to the number of dually labeled molecules.

3.4.5 Western blot

The transgenic HEK 293 cells expressing MOP-eGFP and 5-HT_{1A}-Tomato were cultured in collagen-coated T25 flasks in DMEM medium supplemented with 10 % FBS, PenStrep and 0.4 mg / ml phleomycin D1 antibiotic. Upon reaching 90 % confluence the cell media was exchanged for media supplemented with agonist to MOP (**paper I**) or agonists to MOP and/or 5-HT_{1A} (**paper 2**). After 18 h incubation the adherent cells were removed from the flasks with trypsin-EDTA (0.05 %, Thermo Scientific), washed with ice cold PBS and centrifuged at 1500 rpm for 5 min at 4 °C. The cell pellets were solubilized in RIPA lysate buffer ($10x10^6$ cells / ml, Sigma-Aldrich) containing protease inhibitor and phosphatase inhibitor (Sigma-Aldrich) and incubated for 30 min on ice. The cell solution was transferred to Eppendorf tubes and centrifuged at 10 000 rpm for 10 minutes. Total protein concentration was established for every sample with a colorimetric essay from BioRad RC DC Protein Assay (Bio-Rad). 20 µg of protein from each treatment was diluted to 30 µl with mili-Q water and denatured at 70 °C for 10 min with 4X LDS Sample Buffer, 10X Sample Reducing Agent (Invitrogen). Samples were loaded on precast polyacrylamide gels (Invitrogen) along with 5 µl pre-stained protein ladder (Thermo Scientific), electrophoresed and transferred onto a nitrocellulose membrane (Thermo Scientific). The membrane was probed over night with mouse α-ERK1/2, rabbit α-Phospho-ERK1/2, mouse α-β-actin (Invitrogen), mouse α-p38 and mouse α-Phospho-p38 (CellSignaling). Only one primary antibody was used at a time and the membrane was stripped for 15 min with Western blot stripping buffer (Thermo Scientific) in-between the different primary antibodies. Depending on type of primary antibody, either biotin or horseradish peroxidase conjugated secondary antibody (Invitrogen) was used for detection.

3.5 DATA REPRESENTATION AND STATISTICAL ANALYSIS

Student's t-test was used to determine whether the difference between the mean values measured are significantly different from each other. The results are reported using a two-tailed P-value (P). P = 0.05 is used as the cutoff for significance. Calculations were performed in OriginPro 2018 (OriginLab Corporation, USA). Graphs and figures were generated using OriginPro 2018 and Adobe Photoshop CC (Adobe Systems Incorporated, USA)

3.6 CALCULATING THE APPARENT DISSOCIATION CONSTANT

The apparent dissociation constant for MOP-eGFP and 5-HT1A-Tomato binding can be derived as follows:

$$K_d = \frac{[MOP-eGFP]_{free} \cdot [5-HT1A-Tomato]_{free}}{[MOP-eGFP-5-HT1A]}, \quad (13)$$

where [MOP-eGFH]$_{free}$ and [5-HT$_{1A}$-Tomato]$_{free}$ are concentrations of free receptors, MOP-eGFP and 5-HT$_{1A}$-Tomato, respectively, and [MOP-eGFP–5-HT1A-Tomato] is the concentration of receptor-receptor complexes.

For both receptors, MOP-eGFP and 5-HT1A-Tomato, the concentration of free receptor molecules can be expressed as the difference between the total concentration and the concentration of receptor-receptor complexes, rendering equation (6a) into:

$$K_d = \frac{([MOP-eGFP]_{total} - [MOP-eGFP-5-HT1A]) \cdot ([5-HT1A-Tomato]_{total} - [MOP-eGFP-5-HT1A])}{[MOP-eGFP-5-HT1A]} \quad (14)$$

If we divide both, the numerator and the denumerator in eq. (6b) by the total concentration of red-labeled molecules:

$$K_d = \frac{\frac{([MOP-eGFP]_{total} - [MOP-eGFP-5-HT1A]) \cdot ([5-HT1A-Tomato]_{total} - [MOP-eGFP-5-HT1A])}{[5-HT1A-Tomato]_{total}}}{\frac{[MOP-eGFP-5-HT1A]}{[5-HT1A-Tomato]_{total}}}, \quad (15)$$

and rearrange eq. (15), the following expression is obtained:

$$K_d = \frac{([MOP-eGFP]_{total} - [MOP-eGFP-5-HT1A]) \cdot \left(1 - \frac{[MOP-eGFP-5-HT1A]}{[5-HT1A-Tomato]_{total}}\right)}{\frac{[MOP-eGFP-5-HT1A]}{[5-HT1A-Tomato]_{total}}}. \quad (16)$$

By expressing the molar concentration in terms of the average number of molecules in the OVE, c = n/V$_{OVE}$, where n is the number of moles, n = (N/N$_A$), eq. (16) becomes:

$$K_d = \frac{\left(\frac{N_g^{total}}{N_{A \cdot V_{OVE}}} - \frac{N_{gr}}{N_{A \cdot V_{OVE}}}\right) \cdot \left(1 - \frac{N_{gr}}{N_r^{total}}\right)}{\frac{N_{gr}}{N_r^{total}}}, \quad (17)$$

which after introducing RCCA = $\frac{N_{rg}}{N_r^{total}}$, gives:

$$K_d = \frac{(N_g^{total} - N_{gr}) \cdot \frac{1}{N_{A \cdot V_{OVE}}} \cdot (1 - RCCA)}{RCCA} = = \frac{(N_g^{total} - N_r^{total} \cdot RCCA) \cdot (1 - RCCA)}{RCCA} \cdot \frac{1}{N_{A \cdot V_{OVE}}} \quad . \quad (18)$$

4 RESULTS

4.1 OPIOIDS DIFFER IN THEIR ABILITY TO POTENTIATE HETERODIMER FORMATION BETWEEN MOP AND 5-HT$_{1A}$ AND AFFECT SECOND MESSENGER SYSTEM DIFFERENTLY (PAPER I)

Non-peptide opioids potentiate MOP and 5-HT$_{1A}$ heterodimerization to a different extent. CLSM imaging showed clear co-localization of both receptors, MOP-eGFP and 5-HT$_{1A}$-Tomato, in the plasma membrane in both, the HEK 293 and the PC12 cells (Fig. 4B). It also showed that treatment with non-peptide opioids did not cause internalization, neither of individual receptors, nor of receptor heterodimers. This is in contrast with the effect caused by treatment with the opioid peptide DAMGO, which promoted MOP internalization, but not internalization of the MOP-eGFP–5-HT$_{1A}$-Tomato heterodimers.

FCCS analysis, performed on cells selected to express similar levels of both receptors, $N_{MOP} = (27 \pm 6)$ and $N_{5\text{-}HT1A} = (25 \pm 3)$, corresponding to an average concentrations of: $c_{MOP} = (320 \pm 70)$ nM and $c_{5\text{-}HT1A} = (300 \pm 40)$ nM, respectively, showed that MOP-eGFP and 5-HT$_{1A}$-Tomato receptors not only co-localized in the plasma membrane, but also formed heterodimers, as evidenced by tCCCs. On average about 33 % (RCCA = 0.33) of the 5-HT$_{1A}$-Tomato receptors were bound in heterodimer complexes with MOP-eGFP in untreated cells. From these measurements, an apparent dissociation constant for the heterodimers was determined, $K_d^{app} = (440 \pm 70)$ nM.

Moreover, FCCS showed that treatment with different concentrations of fentanyl increased the number of heterodimers between MOP-eGFP and 5-HT$_{1A}$-Tomato (Fig. 5A and B). Fentanyl treatment had a dose dependent increase in heterodimers, as evident from the increase in RCCA from $RCCA_{Fentanyl}^{50\ nM} = 0.42 \pm 0.09$, which was not significantly different from the RCCA value measured in untreated cells (P = 0.067), to $RCCA_{Fentanyl}^{500\ nM} = 0.49 \pm 0.09$ (P = 0.028) in cells treated with 500 nM fentanyl, and $RCCA_{Fentanyl}^{750\ nM} = 0.62 \pm 0.07$ (P = 3.16E-7) in cells treated with 750 nM fentanyl. From the experimentally determined concentration of heterodimers and the known concentration of fentanyl, the effect of fentanyl on the extent of MOP-eGFP and 5-HT$_{1A}$-Tomato heterodimerization could be quantified (Fig. 5B, solid red line). Considering the concentration of heterodimer complexes as a dependent variable, the concentration of fentanyl as an independent variable and assuming no competing reactions, the concentration of fentanyl at which the number of heterodimers would be doubled was

determined to be (1.90 ± 0.05) μM [105]. Unexpectedly, treatment with 1 μM fentanyl showed a decrease, rather than the expected increase in the concentration of heterodimers (Fig. 5B, dashed red line) and the RCCA decreased to 0.45 (SD = 0.11, P = 0.004). This suggested that other processes, such as receptor homodimer formation and/or higher-order receptor heterooligomer formation may occur at high fentanyl concentrations [106] and/or that fentanyl at such high concentrations may be toxic to cells [107].

With this in mind, no concentrations higher than 750 nM were investigated and this concentration was selected in further studies to compare the effects of different opioids. FCCS showed that for treatment with 750 nM: fentanyl, the RCCA was $RCCA_{Fentanyl}^{750\ nM}$ = 0.62 ± 0.07, which was significantly different from the RCCA value measured in untreated cells (P = 3.16E-7); $RCCA_{Morphine}^{750\ nM}$ = 0.47 ± 0.08 (P = 1.65E-4); $RCCA_{Codeine}^{750\ nM}$ = 0.59 ± 0.07 (P = 5.25E-7) and $RCCA_{Oxycodone}^{750\ nM}$ = 0.47 ± 0.09 (P = 0.0117) (Fig. 5C). Moreover, the RCCA value measured for cells treated with fentanyl was significantly higher than that measured in cells treated with equimolar concentrations of morphine (P = 2.48E-4) or oxycodone (P = 6.99E-4), but not significantly higher than that for codeine (P = 0.24). The difference in RCCA values measured in cells treated with codeine was significantly higher than that in cells treated by morphine (P = 3.66E-3). Based on these measurements and using eq. (14), the apparent dissociation constants for the MOP-eGFP–5-HT_{1A}-Tomato heterodimers in the presence of equimolar concentrations (750 nM) of different non-peptide opioids could be determined: $K_{d,Fentanyl}^{app}$ = (80 ± 70) nM, $K_{d,Morphine}^{app}$ = (200 ± 70) nM, $K_{d,Codeine}^{app}$ = (100 ± 70) nM and $K_{d,Oxycodone}^{app}$ = (200 ± 70) nM. Likewise, the apparent heterodimer dissociation constants in the presence of different concentrations of fentanyl were determined to be: $K_{d,50\ nM\ Fentanyl}^{app}$= (260 ± 70) nM, $K_{d,500\ nM\ Fentanyl}^{app}$= (180 ± 70) nM, $K_{d,750\ nM\ Fentanyl}^{app}$= (80 ± 70) nM, and $K_{d,1\ \mu M\ Fentanyl}^{app}$= (220 ± 70) nM.

Treatment with non-peptide opioids increase to a different extent the brightness of eGFP and Tomato. Prolonged treatment with non-peptide opioids increased eGFP brightness, as evident from the measured counts per second and per molecule (CPM). In untreated cells, average eGFP brightness was $CPM_{Untreated}^{eGFP}$ = (1.1 ± 0.3) kHz. In treated cells, eGFP brightness nearly doubled, showing statistically significant difference for all treatments: $CPM_{Fentanyl}^{eGFP}$ = (1.9 ± 0.7) kHz (P = 0.015), $CPM_{Morphine}^{eGFP}$ = (2.0 ± 0.5) kHz (P = 9.6E-3), $CPM_{Codeine}^{eGFP}$ = (1.9 ± 0.5) kHz (P = 5.8E-3), and $CPM_{Oxycodone}^{eGFP}$ = (1.8 ± 0.7) kHz (P = 0.027). Interestingly, an increase in Tomato brightness was also observed in cells treated with 750 nM

fentanyl or morphine, but not in cells treated with codeine or oxycodone. However, the increase in Tomato brightness was not as pronounced as for eGFP, and changed from $CPM_{Untreated}^{Tomato}$ = (0.8 ± 0.2) kHz in untreated cells to: $CPM_{Fentanyl}^{Tomato}$ = (1.1 ± 0.3) kHz (P = 0.021) for treatment with 750 nM fentanyl; $CPM_{Morphine}^{Tomato}$ = (1.3 ± 0.3) kHz (P = 3.0E-3) for treatment with 750 nM morphine, whereas it remained unchanged (within the limits of the experimental error) for treatment with 750 nM codeine, $CPM_{Codeine}^{Tomato}$ = (1.0 ± 0.3) kHz (P = 0.20), or 750 nM oxycodone, $CPM_{Oxycodone}^{Tomato}$ = (0.9 ± 0.3) kHz (P = 0.12). It is hard to say with certainty why the brightness of fluorescence reporters has changed following treatment with non-peptide opioids, two potential processes: receptor homodimerization and fluorescence lifetime change due to environmental changes during signal transduction, can independently and jointly cause such effects.

Non-peptide opioids differ in the extent to which they activate major signal transduction pathways. In order to assess the effects of non-peptide opioids on the second messenger pathways in HEK 293 cells expressing MOP-eGFP and 5-HT_{1A}-Tomato, phosphorylation of MAPKs ERK1/2 and p38 was investigated. MOP activation has been shown to trigger phosphorylation of both, ERK1/2 [108] and p38 [109]. Western blot analysis showed an increase in phosphorylated ERK1/2 and p38 in cells that had been treated with 750 nM of morphine, oxycodone, codeine or fentanyl, when compared to untreated cells (Fig. 5D and E). Fentanyl elicited the strongest ERK1/2 activation (mean = 1.156, SD = 0.183, P = 8.52E-4), while oxycodone barely activated it (mean = 0.506, SD = 0.139, N.S). In contrast, oxycodone elicited the strongest p38 activation (mean = 1.441, SD = 0.517, P = 0.025), while the effects of fentanyl, morphine, and codeine were similar. Interestingly, LC-MS/MS metabolite analysis indicated that these effects are likely attributed to the primary non-peptide opioid compounds in their own right, as there were no common opioid metabolites detected neither in the cell culture medium nor in the cell lysate.

Non-peptide opioids elicit different intracellular Ca^{2+} signaling dynamics. Time-lapse CLSM imaging of intracellular Ca^{2+} levels using the cell-permeant Fura Red ratiometric dye showed that stimulation with equimolar concentration of different non-peptide opioids acutely induced different changes in the intracellular Ca^{2+} levels in HEK293 cells expressing MOP-eGFP and 5-HT_{1A}-Tomato (Fig. 5F). In untreated cells, intracellular Ca^{2+} showed no fluctuations in concentration. Following addition of 750 nM morphine, the stationary state levels did not change, but the stationary state appeared to have lost its stability and sinusoidal oscillations in Ca^{2+} levels with smoothly increasing amplitudes and a period of about 5 min, emerged.

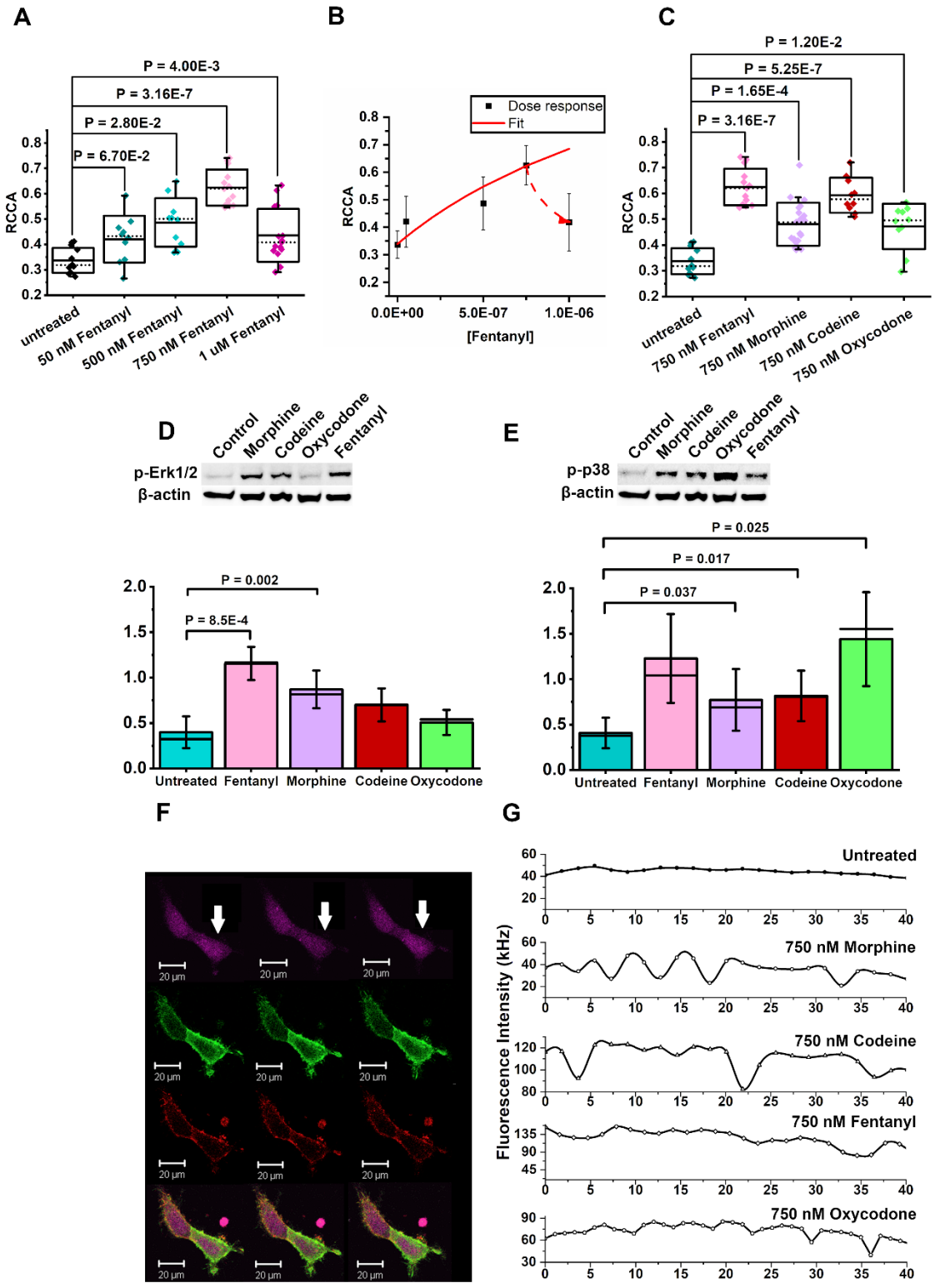

Figure 5. Results from non-peptide opioid study in HEK 293 cells expressing MOP-eGFP and 5-HT$_{1A}$-Tomato (paper I) A) RCCA analysis shows that prolonged treatment (18 h) with fentanyl induces a dose-dependent increase in MOP-eGFP and 5-HT$_{1A}$-Tomato heterodimer formation. For fentanyl concentrations above 1 µM, the extent of heterodimer formation drops. **B)** Fentanyl dose response curve calculated from the experimentally obtained RCCA values in A and the known concentrations of Fentanyl. **C)** Prolonged treatment with non-peptide opioid drugs at 750 nM promotes hetero dimer formation between MOP-eGFP and 5-HT$_{1A}$-Tomato, as evident by the recorded RCCA. **D)** Western blot analysis shows that prolonged treatment with non-peptide opioids activates ERK1/2 signaling pathways differently. **E)** p38 activation varies after prolonged exposure to non-peptide opioids, as evident by western blot analysis. **F)** CLSM time-lapse imaging of Ca^{2+} levels (Fura Red, dark violet) in HEK293 cells expressing MOP-eGFP (green) and 5-HT1A-Tomato (red) after 40 min treatment with 750 nM oxycodone. White arrows indicate changes in Fura Red fluorescence intensity, reflecting

changes in the concentration of Ca^{2+} ions. Scale bar 20 µm. **G)** Fluctuations in Fura Red fluorescence intensity over time following initial treatment with 750 nM of non-peptide opioid drugs. The box-and-whisker Plot (A and C): the solid line shows the mean value, the dashed line shows the median, box represents the standard deviation and the whiskers give the 5-95 percentile. The staple-whisker plots (D and E): staples show the mean value, the solid line the median and the whiskers the standard deviation. All statistical analysis are two-tailed P-value (P) with P = 0.05 used as the cutoff for significance.

Treatment with 750 nM codeine caused a pronounced increase in Fura Red fluorescence intensity, indicating that intracellular Ca^{2+} levels have decreased, and induced oscillations in intracellular Ca^{2+} levels. However, these oscillations showed features of so-called relaxation oscillations [110], which are characterized by a relatively long relaxation period during which the system remained in the stationary state, alternating with a short period in which abrupt decrease in fluorescence intensity, i.e., increase in intracellular Ca^{2+} level was observed. Treatment with 750 nM fentanyl did not cause any oscillations in intracellular Ca^{2+} levels, but a four-fold increase in Fura Red fluorescence intensity was noted, indicating that intracellular Ca^{2+} levels decreased markedly following fentanyl addition. Finally, treatment with 750 nM oxycodone increased somewhat Fura Red fluorescence intensity, and small-amplitude relaxation oscillations with gradually increasing amplitudes and a period of about 5 min were observed (Fig. 5G).

4.2 5-HT$_{1A}$ AGONISTS ABOLISH MORPHINE INDUCED MOP AND 5-HT$_{1A}$ HETERODIMERS (PAPER II)

After establishing that chronic exposure to non-peptide opioid drugs did potentiate the formation of MOP-eGFP and 5-HT$_{1A}$-Tomato heterodimers, the objective was to see how treatment with 5-HT$_{1A}$ agonists would affect these interactions. For this study, morphine was used to potentiate heterodimer formation between MOP-eGFP and 5-HT$_{1A}$-Tomato. Five agonists to 5-HT$_{1A}$ were chosen, namely serotonin (5-HT), buspirone and three novel drug candidates that are analogs to buspirone (Fig. 6).

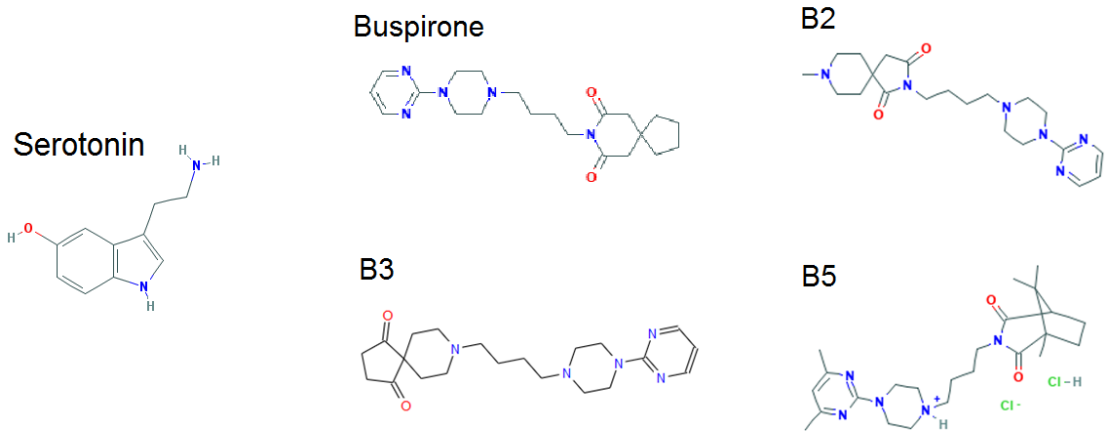

Figure 6. **5-HT$_{1A}$ partial agonists: Serotonin** 3-(2-Aminoethyl)-1H-indol-5-ol, **Buspirone** (8-[4-(4-pyrimidin-2-ylpiperazin-1-yl)butyl] -8-azaspiro[4.5] decane-7,9-dione), **B2** (8-methyl-2-{4-[4- (pyrimidin-2-yl) piperazin-1-yl] butyl}-2,8-diazaspiro [4.5] decane-1,3-dione), **B3** (8-{4-[4-(pyrimidin-2-yl) piperazin-1-yl] butyl} -8-azaspiro[4.5] decane-1,4-dione) and **B5** (3-[4-[4-(4,6-dimethylpyrimidin-2-yl) piperazin-1-ium-1-yl] butyl]-5,8,8-trimethyl -3-azabicyclo[3.2.1] octane-2,4-dione;chloride;hydrochloride

As before, CLSM imaging showed co-localization of the receptors on the plasma membrane with neither of the compounds inducing internalization. In accordance with paper I, FCCS measurements showed an increase in the average number of heterodimer complexes in cells treated with 750 nM of morphine for 18 h. Treatment with 750 nM of 5-HT or buspirone reduced the average number of MOP-eGFP-5-HT_{1A}-Tomato heterodimers, as compared to untreated cells, however, only the decrease from the buspirone cohort showed statistical significance. Moreover, FCCS analysis showed that co-treatment with equimolar concentrations (750 nM) of morphine and 5-HT_{1A} agonists significantly reduced the number of MOP-eGFP-5-HT_{1A}-Tomato heterodimers, as compared to cells treated with 750 nM of morphine. Albeit to different extents, with the novel busprione analog B2 significantly reducing the average number of heterodimers to 21 %, in the presence of equimolar concentrations of morphine, which was the lowest RCCA value calculated for any treatment cohort, including untreated (Fig. 7A). Brightness (CPM) analysis showed that treatment with 5-HT, morphine and co-treatment with equimolar concentrations of 5-HT and morphine significantly increased the brightness of eGFP (Fig. 7B). Whereas, 5-HT, morphine, buspirone and co-treatment with morphine and 5-HT or busprione significantly increased the brightness of Tomato (Fig. 7C).

Western blot analysis of ERK1/2 and p38 MAPK signaling showed that all treatment strategies increased the phosphorylation of both ERK1/2 and p38, to different extents. Treatment with buspirone, B2, B3 and B5 had a significant increase in ERK1/2 activation, as had co-treatment with morphine and busprione or B2. Moreover, significant activation of p38 was observed in cells treated with 5-HT and busprione, as well as in cells co-treated with morphine and 5-HT.

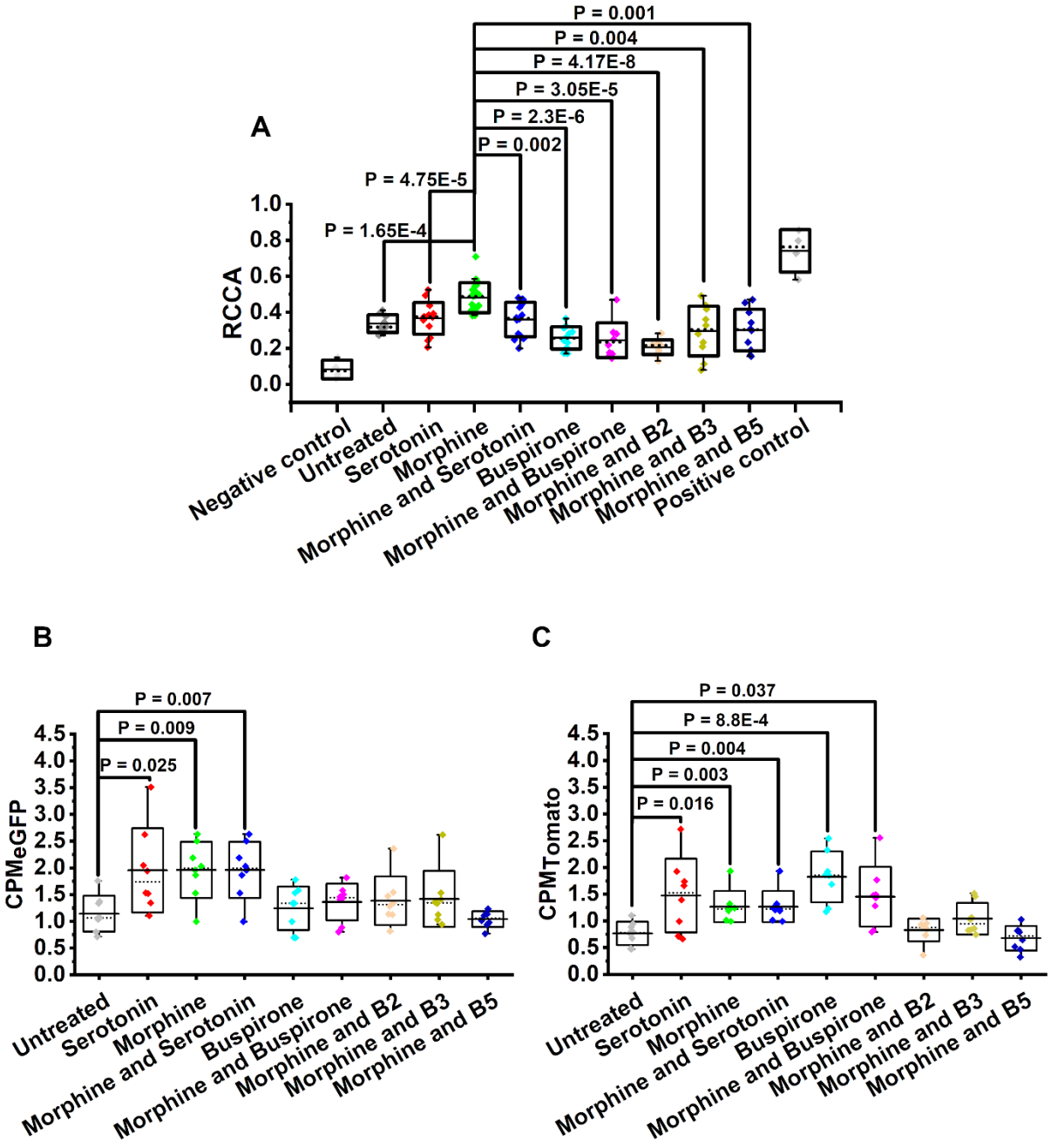

Figure 7. Results from dual agonist study in HEK 293 cells expressing MOP-eGFP and 5-HT$_{1A}$-Tomato (paper II) A) RCCA data shows that treatment with either or both 5-HT$_{1A}$ or MOP agonist at 750 nM significantly changes the number of heterodimer complexes between the receptor, as compared to untreated cells. Additionally, all RCCA values recorded fall within the negative and positive FCCS controls. **B)** Brightness analysis (CPM) of eGFP from the same measurements as in A show an increase in eGFP brightness for treatment with serotonin, morphine and co-treatment with morphine and serotonin. **C)** Brightness analysis of Tomato from the same measurements as in A show an increase in brightness for all treatment cohorts except co-treatment with morphine and novel buspirone analogs: B2, B3 and B5.

4.3 OPIOID RECEPTORS ARE LARGLEY EXCLUDED FROM GM1 GANGLIOSIDE-ENRICHED DOMAINS (PAPER III)

In this study, two different FCCS approaches were applied to study the dynamics between GM1 ganglioside-enriched domains and opioid receptors. Namely, the interactions between MOP-Tomato and BODIPY® FL C5-ganglioside GM, in transfected PC12 cells and PC12 cells expressing MOP-eGFP and the GM1-specific cholera toxin B subunit conjugated with Alexa Fluor® 647 (CTxB-AF647). FCCS measurements on PC12 cells expressing MOP-Tomato showed no interaction between the receptor and BODIPY® FL C5-ganglioside GM. Similarly, no interaction was detected in PC12 cells between MOP-eGFP and CTxB-AF647. In addition, FCCS was also applied to quantitatively characterize the interactions between BODIPY® FL C5-ganglioside GM and CTxB-AF647 in solution and on live PC12 cells. The solution measurements yielded an apparent equilibrium constant K_d = (2±1) µM, while the PC12 cell measurements produced a RCCA value which, when compared to positive and negative FCCS control PC12 cells, indicated significant binding between the two compounds. FCCS control cells were generated by transfecting cells to express either freely diffusing eGFP and Tomato (negative control) or eGFP-Tomato heterodimers (positive control). Although first introduced in this paper, the FCCS positive and negative control cells were used as controls in both paper I and II. To ensure that fluorescence labeling did not affect the function of the opioid receptors, both MOP and KOP (kappa opioid receptor) where expressed in PC12 cells with eGFP genetically fused to the N-terminal (previous experiments had C-terminal eGFP tag). Comparison of long and short decay times showed no significant difference regarding labeling site on MOP and KOP receptors (Fig. 8).

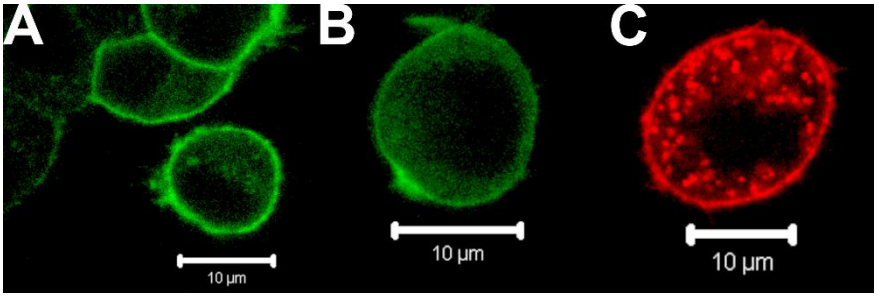

Figure 8. Expression of MOP in PC12 cells. A) MOP with C-terminal eGFP tag. **B)** MOP with N-termial eGFP tag. **C)** MOP with C-terminal Tomato tag. All scale bars 10 µm.

4.4 THE DYNAMIC EQUILIBRIUM BETWEEN MONOMERIC, OLIGOMERIC AND AGGREGATED FROM INFLUENCE THE EFFICACY OF CELL-PENETRATING PEPTIDES (PAPER IV)

In this study, FCS was first applied to map the dynamics of the cell-penetrating peptide PepFect 14 (PF14). Measurements with FCS, in solution, showed that PF14K-CR6G (FP14 conjugated with carboxyrhodamine 6G) had a propensity to self-associate into oligomers and aggregates, that where four orders of magnitude larger than the monomers. FCS also revealed that the process of PF14K-CR6G self-association was dependent on protonation (pH) and concentration. Additionally, FCS measurements performed on the apical plasma membrane of live PC12 cells and in their surrounding solution showed that PF14K-CR6G accumulated on the plasma membrane over time, which was also confirmed via CLSM imaging, and exhibited a wider range of differently sized oligomers on the plasma membrane, as compared to solution. Finally, FCS measurements revealed that the diffusion time of Cy5 labeled small interfering RNA (Cy5-siRNA) increased with the increase in PF14 concentration. The interaction between Cy5-siRNA and PF14K-6G was further probed via FCCS, which showed that Cy5-siRNA and PF14K-6G more readily formed complexes on the plasma membrane of live PC12 cells than in solution.

4.5 CARBOHYDRATE EPITOPES INFLUENCE PROTEIN UPTAKE OVER THE PLASMA MEMBRANE

Galactose-α-1,3-galactose (α-Gal) presenting bovine serum albumin (BSA) was found to be more readily absorbed by immature monocyte-derived dendritic cells (iMDDCs), than BSA without α-Gal. CLSM imaging of fixed iMDDCs showed the presence of Alexa Fluor® 488 conjugated BSA- α-Gal in cytoplasmic vesicles, both after 1 and 4 h incubation. Whereas, incubation with Alexa Fluor® 488 conjugated BSA showed no signs of vesicle formation in fixed iMDDCs, after 1 and 4 h. The results corroborated data acquired via flow cytometry, which indicated that carbohydrate epitopes are more important for uptake than protein size. This was shown by comparing the uptake of BSA- α-Gal and bovine thyroglobulin (bTG) in iMDDCs from healthy individuals. Despite bTG having a molecular weight almost ten times that of BSA- α-Gal no differences in uptake could be observed.

5 DISCUSSION

The ever-growing advances in the field of fluorescence microscopy have allowed scientists to quantitatively and with high precision elucidate many of the molecular interactions that underlie the complex dynamic of a living cell [111-113]. In my work, one such technique was predominantly used, the quantitative time-resolved fluorescence technique with single molecule sensitivity called Fluorescence Correlation Spectroscopy (FCS) and its dual color version Fluorescence Cross-Correlation Spectroscopy (FCCS).

FCCS was fundamental in testing the hypothesis that prolonged exposure to non-peptide opioid drugs promoted heterodimer formation between MOP and 5-HT_{1A}[66]. The high spatial and temporal resolution of FCCS, coupled to it being for most parts a non-destructive technique made it possible to quantitatively characterize the interactions between the two receptors in live cells, as well as the effects of the most commonly used non-peptide opioid drugs: morphine, oxycodone, codeine and fentanyl, on the extent of these interactions (**Paper I**). Calculation of the RCCA revealed that on average around 33% (RCCA = 0.33) of 5-HT_{1A}-Tomato receptors had formed heterodimer with MOP-eGFP. This value might not be physiologically relevant and might only apply to this cell model, with its expression level, where the average concentration of (270 ± 60) nM for MOP-eGFP and (250 ± 30) nM for 5-HT_{1A}-Tomato. Transfecting cells to express proteins of interest through powerful promotors does lead to strong over-expression. However, this is usually a transient effect. Stably transformed cells do not yield as high expression as transiently transfected cells, which is why only stable cell lines where investigated (**paper I and II**). Moreover, all non-peptide opioid drugs were found to significantly increase the number of MOP and 5-HT_{1A} heterodimer complexes, with fentanyl showcasing the strongest contribution to the heterodimer formation between the receptors. Although, the concentrations of 750 nM fentanyl might be relatively high, given that fentanyl achieves analgesic effect at around 1.8 – 4.4 nM (blood plasma concentration), in opioid-naive postoperative patients [114]. It is important to point out that treatment for cancer pain measured concentrations as high as 530 nM in patients [107], thus placing the concentrations used in this study in a physiologically relevant range. Moreover, in this study only equimolar concentrations of opioids where compared. We did not consider equipotent concentrations of opioids. Although there are several conversion tables for opioids, they are perceived as unreliable [115]. The few studies that have addressed opioid equianalgesic dose/potency ratios are heterogeneous in regards to size, subjects, specific aims, settings and study method [116]. Rennick et al. concluded from their findings that there is no true universal way to accurately perform

equianalgesic conversions for opioids [117]. Morphine and codeine showed significant differences in their potency to stabilize MOP–5-HT_{1A} heterodimers. Surprisingly, exposure to codeine had an average stronger effect than morphine, both in regards to heterodimer formation and changes in calcium signaling dynamics. An observation that is contrary to the general view that codeine is an inactive prodrug with a low affinity for MOP, with analgesic effect only after metabolic conversion to morphine [118-120] and dihydrocodeine-6-O-gluconoride [121,122]. Codeine as an active substance is in line with the fact that HEK 293 cells do not express the CYP2D6 gene (https://www.proteinatlas.org/ENSG00000100197-CYP2D6/cell, 2019-10-10) needed to metabolize codeine [123]. LC-MS/MS analysis showed that there were no traces of codeine metabolites, neither in the cell medium nor in the cell lysates. The analysis of the cell medium showed the presence of codeine, but the analysis of cell lysate failed to measure any compound. This was most likely due to the minute quantities of drugs present in cell lysate. The opioid-induced increase in heterodimer interactions between MOP-eGFP and 5-HT_{1A}-Tomato might alter intracellular signaling and might contribute to neuroplastic changes previously linked to chronic pain [124]. The activation of presynaptic MOP and 5-HT_{1A} can in a cooperative manner inhibit the release of GABA onto the periaqueductal gray (PAG) [1]. Activation of the $GABA_A$ receptors in neurons projecting into the PAG exhibits a net pronociceptive effect [125]. Thus, the opioid induced heterodimer formation between MOP and 5-HT_{1A} could hamper GABA release by rendering both receptors inactive. Which could potentially promote pronociceptive pathways via $GABA_A$ receptors.

While prolonged exposure to MOP agonists seems to induce receptor heterodimerization the opposite effect was observed for prolonged exposure with 5-HT_{1A} agonists, particularly the novel busprione analog B2 (**paper II**). B2 has a similar structure to buspirone, with a key difference being an additional nitrogen atom on B2. According to the QSAR model, the charge associated with nitrogen adds significant influence on the activity of the compound, which is in line with the obtained FCCS data. Additional structural differences between buspirone and B2 are the potential to form additional hydrogen bonds, compound bulk properties and spatial polarity, which all might influence the overall performance of the compound. Brightness analysis (CMP) showed a significant two-fold increase in Tomato brightness in the cells treated with serotonin and buspirone, as well as for cells co-treated with morphine and serotonin or busprione. Potentially, this can be explained by agonist-induced 5-HT_{1A} homodimerization, although further studies would be needed to confidently draw that conclusion. In accordance with our hypothesis, we demonstrated that prolonged (18h) morphine exposure induced heterodimer formation between MOP-eGFP and 5-HT_{1A}-Tomato could be relaxed by co-administrating an agonist to 5-HT_{1A}. The diminished degree of measurable MOP and 5-HT_{1A}

heterodimers, in the presence of morphine and any of the tested 5-HT_{1A} agonists, suggest that activation of 5-HT_{1A} is a potential key mechanism in preventing adverse effects of prolonged opioid treatment. Buspirone has been shown to counteract OIH and reverse opioid tolerance and the rewarding effects of opioids in animal trials [67-69]. Haleem et al suggested that this was due to buspirones agonistic effects on 5-HT_{1A} and antagonistic effects on dopamine D2 receptor [67].

The hypothesis formulated by Kosek et al. suggested that sensitization of pronociceptive pathways could be caused by the heterodimer formation between MOP and 5-HT_{1A}. Which could contribute to changes in neuroplasticity, via altered cellular signaling. In the HEK 293 cell model, changes in cell signaling were observed for prolonged exposure to all non-peptide opioids tested (**paper I**). Fentanyl elicited the highest activation of the ERK1/2 pathway and a notable activation of p38, whiles acutely decreasing intracellular calcium levels. Notably, oxycodone had the weakest, although significant, increase in heterodimer complexes, but the strongest activation of the p38 MAPK pathway. This finding is in line with the observation that rats exhibited increased p38 activity during chronic oxycodone exposure [126] and that opioid reward behavior was modulated by p38 activation in mice [127], while KOP induced p38 activation was found to reinstate drug seeking behavior in mice [128]. Activation of p38 could be very relevant for the observed adverse and addictive qualities of oxycodone, as a recent study argued that the addictive qualities of oxycodone outweighed its benefits as a prescription drug[129].

Both morphine and buspirone have been shown to activate MAPK signaling pathways [130-133]. Therefore, it is reasonable to expect a higher concentration of phosphorylated ERK1/2 and p38 in all treatment cohorts as compared to the untreated (**paper II**). The activation of EK1/2 has been linked to opiate addiction [133] and activation of p38 has been proven instrumental in MOP internalization and maintenance of MOP heterodimers [109]. Prolonged morphine use has been shown to induce changes at the receptor level and alter CREB activation through MAPK/ERK, leading to adverse opioid effects [131]. In addition, morphine has been found to increase ERK phosphorylation via a dopamine D1 receptor dependent mechanism [67]. Dopamine D1 receptors are known to modulate dopamine D2 receptor dependent events [134], which could potentially be one of the mechanisms through which buspirone reverses adverse opiate effects, as suggested by Haleem et al., although further research would be needed to fully map the extent of these interactions.

The picture that emerges is that the dynamics of GPCR-interactions on the plasma membrane are of paramount importance for complex biological processes, like pain

modulation. One key aspect of the plasma membrane explored in this thesis it the feature of compartmentalization (**paper III**). Compartmentalization allows physical separation of molecules via inclusion / exclusion from specific domains. Which in turn affects their local concentration, chemical equilibrium and interaction kinetics. FCS and FCCS measurements elucidated a model for MOP organization, which saw it associate with cholesterol and GPI-enriched domains whiles being excluded from GM1 ganglioside-enriched domains. In contrast, 5-HT_{1A} has been shown to associate with GM1 enriched domains [135] whiles, treatment with exogenous ganglioside GM1 was found to beneficially modulate dopamine and serotonin, and restore normal levels of glutamate and GABA [136]. Hypothetically, the heterodimerization between MOP and 5-HT_{1A}, resulting from prolonged opioid exposure, could hinder 5-HT_{1A} from associating with GM1 enriched domains, which could potentially also negatively affect pain modulation. Although, this hypothesis would need to be thoroughly tested before any such conclusion could be confidently drawn.

It is clear that innovative approaches are needed for the treatment of chronic pain. One such approach, recently published, utilized p38-siRNA loaded nanoparticles to significantly alleviate allodynia and reduce microgliosis in rats [137]. For such therapies to become well established the dynamics of how these nanoparticles interact with cells needs to be well characterized. By utilizing FCS / FCCS we successfully characterized how cell-penetrating peptide-nanoparticles interacted with the plasma membrane of live cells and how chemical factors like pH and concentration affected their self-assembly. We also mapped to a good extent the interaction of these nanoparticles with siRNA (**paper IV**). This research project highlighted the great versatility of FCS / FCCS. By employing different labeling strategies targeting either PF14, siRNA or both the diffusion properties of PF14 as well as interactions between PF14 and the plasma membrane or siRNA could be elucidated. How molecules like PF14 self-assemble is important to know if they are to be used as oligonucleotide delivery vectors.

Finally, in this thesis we employed the most conventional fluorescence application, namely CLSM to study cellular uptake of red meat allergens (**paper V**). The labeling strategy employed in this study used DAPI, Alexa Fluor® 488 and Alexa Fluor® 555, and while conventional CLSM is well established there are still pitfalls that can severely affect data interpretation. Even though DAPI and Alexa Fluor® 488 are spectrally well separated DAPI can crosstalk into the green channel through a process known as photo conversion, as a result from illumination with UV-light [138]. In addition, Alexa Fluor® 555 is known to be cross-excited by incident light at 485 ± 10 nm [139]. Taking this into consideration when designing a CLSM experiment is paramount for correct imaging. For this study, all of these parameters

where carefully scrutinized in order to correctly portray the biological events underlying red meat allergy.

In summation, throughout this thesis quantitative fluorescence techniques have been employed to characterize GPCR interactions with other GPCRs and their surroundings, which in itself is a notable achievement. GPCR homo/heterodimer complexes have been measured in live cells for a handful of GPCRs, e.g. [111-113,140], even though these interactions are important targets for drug development. However, some limitations of FCS/FCCS are unavoidable and should be discussed. FCS/FCCS cannot account for endogenous non-fluorescent receptors, fluorescent protein miss folding, receptor constructs with irreversibly photobleached fluorophores or with fluorophores residing for various reasons in dark states. These factors can influence calculations derived from measurements. This particular limitation does not impact the conclusions of this thesis negatively since differences between the experimentally measured values are analyzed. Additional validation of FCS/FCCS was also performed by generating positive and negative FCCS control cells (**papers I-III**), which gave insight into the dynamic range of measurable RCCA values from zero to one hundred percent binding. Moreover, investigation into receptor-label binding site verified that the location of the fluorescent protein binding site did not significantly affect the obtained results (**paper III**).

6 CONCLUSIONS AND FUTURE PERSPECTIVES

The work presented in this doctorate thesis focuses on understanding cellular and molecular mechanisms that underlie the development of opioid induced hyperalgesia (OIH), with a particular emphasis on the role of mu-opioid (MOP) and the serotonin 1 A (5-HT_{1A}) receptor heterodimerization. The starting point of our work is the hypothesis that prolonged exposure to non-peptide opioids promotes heterodimer formation between MOP and 5-HT_{1A} receptors and that altered cellular signaling due to receptor heterodimer formation may contribute to neuroplastic changes that, eventually, lead to sensitization of pronociceptive pathways at the organism level.

To challenge this hypothesis, which was formulated based on indirect clinical and preclinical evidence, Fluorescence Cross-Correlation Spectroscopy (FCCS), an advanced analytical method with high temporal resolution and the ultimate, single-molecule sensitivity, was used to quantitatively characterize in live cells interactions between these two G protein-coupled receptors (GPCRs). In line with the formulated hypothesis, the results showed that MOP and 5-HT_{1A} receptors form in the plasma membrane heterodimers with an apparent dissociation constant K_d^{app} = (440 ± 70) nM). Prolonged exposure to all commonly used non-peptide opioids tested: fentanyl, morphine, codeine and oxycodone, facilitated MOP and 5-HT_{1A} heterodimerization and stabilized the heterodimer complexes, albeit to a different extent: $K_{d,Fentanyl}^{app}$ = (80 ± 70) nM), $K_{d,Morphine}^{app}$ = (200 ± 70) nM, $K_{d,Codeine}^{app}$ = (100 ± 70) nM and $K_{d,Oxycodone}^{app}$ = (200 ± 70) nM. The non-peptide opioids differed also in the extent to which they affected the mitogen-activated protein kinases (MAPKs) p38 and the extracellular signal-regulated kinase (Erk1/2), with morphine, codeine and fentanyl activating both pathways, whereas oxycodone activated p38 but not ERK1/2. Moreover, our work showed that acute stimulation with different non-peptide opioids differently affected intracellular Ca^{2+} levels and signaling dynamics.

Furthermore, we showed that morphine-induced heterodimerization of MOP and 5-HT_{1A} can be restrained by co-treatment with buspirone, an agonist at the 5-HT_{1A} receptor, and buspirone analogues identified by virtual screening: B2, B3 and B5, keeping the level of receptor-receptor heterodimers down to values that are characteristic of untreated cells. In fact, buspirone and compound B2 were not only effective in preventing morphine-induced MOP–5-HT_{1A} heterodimerization, but potentiated also the dissociation of the receptor-receptor

complexes bringing the MOP–5-HT_{1A} heterodimer levels down to values below those measured in untreated cells.

In summary, the work conducted under my PhD studies identified MOP–5-HT_{1A} heterodimerization as a possible mechanism through which aversive effects of non-peptide opioids arise under prolonged use, and has led to the identification of three new compounds, buspirone analogs B2, B3 and B5, that may counteract these effects. Further studies are needed to establish whether this mechanism is also effective in live animals/humans and to determine whether combination therapy with opioids and 5-HT_{1A} agonists may become a new strategy to counter opioid induced hyperalgesia and help to preserve the analgesic effects of opioids.

7 ACKNOWLEDGMENTS

To my family: In the mid-eighties, my parents (**Simona and Romeo**) took the brave leap of faith and left everything they knew, so that their children could have a better future. Without their bravery, I would not be here today. Your bravery inspires me to do things that scare me. My sister **Alexandra**, you somehow manage to have career and raise two fantastic kids. I honestly do not know how you do it. You are a true superhero! My grandmother **Teodora**, you always encouraged and supported me. You always let me be me and were the first to call Jonas family, you are eons ahead of your time (for being a Romanian grannie).

My Gotland family: **Barbro**, my second mother! I do not know how you survived raising those three boys (animals). Clearly you did something wright as they are all fantastic. **Ronny**, I get my work ethic inspiration from you. One day I hope to understand what you say, through your thick accent. My brothers, **Patrik**, you have such a beautiful old soul in you. I could sit and talk to you for hours. **Svante**, the fearlessness with which you throw yourself into any new thing should be an inspiration to anyone reading this.

Vladana, it is impossible, I think, to go through five years without ups and downs. I would like to think we have managed to have mostly ups. You are a deep well of knowledge and that never ceases to amaze me. You have a very Balkan sense of humor and I think it adds very much needed spice to CMM.

André, my mentor and my friend! You were always there for me when I needed you. A constant pillar of support. You are an amazing scientist and a beautiful person. From the bottom of my heart thank you!

The group: **Ann**, you are an inspiration in what one can achieve by setting one's mind to and being dedicated. **Agneta**, I do not think there is anyone kinder or more considerate at CMM than you. You are fearless in your determination and I applaud that. **Sho**, your knowledge in your field is only surpassed by your incredible work ethic. **Lars**, thank you for all your guidance through these five years. I hope to be half the scientist you are!

Eva and Camilla, thank you for taking the time to be my co-supervisors. You both are true inspirations of what the future of science should be.

The lab: five years have passed since I first started at CMM and had the privilege to get to know so many amazing and talented people. **Peter**, you were the first sister I got to know at CMM and I adore how you let your freak flag fly! Fatherhood has never looked better on anyone as it does on you. **Natalie**, you are the heart and smile of CMM. Your kindness and hugs can brighten up any day and make one forget all about failed experiments (vroom vroom my little BMW). If Natalie is the smile of CMM then **Caroline** is without a doubt the laughter. Your laughter can fill any lunchroom with such warmth and joy. **Katie**, you are one of my proudest achievements at CMM. Did not take me long to turn you into a gay guy, although the pieces were already there. You are amazing and funny, and you made me fear ever visiting Swansea. **Johanna**, I still cannot believe you managed to do an entire PhD without drinking coffee. Sometimes I wonder what was in that tea. Keep on representing the west coast for the both of us. **Vinko**, you have this magic way about you that really brightens up my day. Never lose that. **Ellen**, you where the fresh breeze that blew through CMM every now and then, in-between clinical rotations. You could always put a smile on my face.

To my chosen family: There are no word to describe how much I love you gurls (but I will try)! You are so much more than just friends. The bond and love we have transcends anything as trivial as nucleotides. You are all my true ride or die bitches!

My Gothenburg family: Erik, you mean so much more to me than I can describe with word. You are the Patsy to my Edwina. Always remember, I have known you longer that your daughter. **Fabian**, how can anyone so tiny be so amazing? I am in awe of your ambition, determination and ingenuity, but mostly I love you for your incredible kindness and strong coffee. **Rob**, no workplace has ever been as fun or will ever be, as the one I shared with you. There is a beautiful whimsy about you that I cannot stop gravitating towards. I look forward to sharing pomegranates under dirty bars with you when we are in our 60s. **Joe**, I do not think there is a kinder person to have ever walked this planet. Your warmth is only surpassed by your quick wit. **Waldean**, such poise, much beauty, just wow. I love to see you move! Thank you for letting me be your slumlord. **Mattias**, we shared five beautiful years together. I will always remember our young wild days as idiot 20-somethings. I am so glad that you are still in my life. Forever my first love!

My Stockholm family: Filipe, if anyone ever needs to understand the meaning of the word empathy I will send them you. You always inspire me to be a kinder and better person. Whatever programming that drives you is flawless! **Jim**, I can always count on you for anything. That is a rare quality and makes the world not feel as scary. Thank you for always being five steps ahead of everyone with me, and seeing that there is method to my madness. **Alex**, the first time we met I called you the dumbest smart person I knew. But you still stuck around (guess I was right). I am glad that you did! My life is better for having you in it. **Andreas**, I love your joy for life and roll with the punches attitude. You are so steadfastly you and I adore that about you. **Kevin**, the sharpest knife in this set of mismatched cutlery. I do not think there is anything you do not know (except how to answer your phone). You influence me more than I dare to admit. **Christian**, you are the much needed stoic palate cleanser from all these loud bitches. There is such power behind your soft-spokenness. You are forever my Småland sister!

My family around the world: Rand, you went to the Harvard of the south, which you will tell anyone regardless of if they asked. You where my first true friend in Stockholm and introduced me to what was to become my family. I love you always. **Tom and Pedro**, the first of the gurls to get hitched. I miss having you two beauties in Stockholm but love following your adventures on the other side of planet earth.

Jonas, I started this thesis writing about you and I intend to finish it writing about you. Much like I started this journey with you supporting me, I look forward to spending the rest of my life with you by my side. I love you now and forever!

8 REFERENCES

1. Kishimoto K, Koyama S, Akaike N. Synergistic μ-opioid and 5-HT1A presynaptic inhibition of GABA release in rat periaqueductal gray neurons. *Neuropharmacology.* 2001;41(5):529-538.

2. Wei F, Guo W, Zou S, Ren K, Dubner R. Supraspinal Glial–Neuronal Interactions Contribute to Descending Pain Facilitation. *The Journal of Neuroscience.* 2008;28(42):10482.

3. Gosselin R-D, Suter MR, Ji R-R, Decosterd I. Glial Cells and Chronic Pain. *The Neuroscientist.* 2010;16(5):519-531.

4. Schaible HG. Peripheral and central mechanisms of pain generation. *Handb Exp Pharmacol.* 2007(177):3-28.

5. Julius D, Basbaum AI. Molecular mechanisms of nociception. *Nature.* 2001;413(6852):203-210.

6. Swieboda P, Filip R, Prystupa A, Drozd M. Assessment of pain: types, mechanism and treatment. *Ann Agric Environ Med.* 2013;Spec no. 1:2-7.

7. Meyr AJ, Steinberg JS. The Physiology of the Acute Pain Pathway. *Clinics in Podiatric Medicine and Surgery.* 2008;25(3):305-326.

8. Basbaum AI, Bautista DM, Scherrer G, Julius D. Cellular and Molecular Mechanisms of Pain. *Cell.* 2009;139(2):267-284.

9. Nicholson B. Differential diagnosis: nociceptive and neuropathic pain. *Am J Manag Care.* 2006;12(9 Suppl):S256-262.

10. Labuz D, Celik MÖ, Zimmer A, Machelska H. Distinct roles of exogenous opioid agonists and endogenous opioid peptides in the peripheral control of neuropathy-triggered heat pain. *Scientific Reports.* 2016;6:32799.

11. Kosek E, Lampa J, Nisell R. *Smärta och inflammation : vid reumatiska sjukdomar och vanliga smärttillstånd i rörelseapparaten.* Andra upplagan ed.

12. Moore RA, Chi CC, Wiffen PJ, Derry S, Rice AS. Oral nonsteroidal anti-inflammatory drugs for neuropathic pain. *The Cochrane database of systematic reviews.* 2015(10):CD010902.

13. Manglik A, Kruse AC, Kobilka TS, et al. Crystal structure of the [micro]-opioid receptor bound to a morphinan antagonist. *Nature.* 2012;485(7398):321-326.

14. Smith H, Elliott J. Alpha(2) receptors and agonists in pain management. *Curr Opin Anaesthesiol.* 2001;14(5):513-518.

15. Kumar A, Pottabathini R, Bhatnagar A, Garg S, Gupta V. Pharmacological Management of Neuropathic Pain: Current Trends and Possible Approaches. *Archives of Neuroscience.* 2017;4(1):13.

16. Baron R. Mechanisms of Disease: neuropathic pain[mdash]a clinical perspective. *Nat Clin Pract Neuro.* 2006;2(2):95-106.

17. Yam MF, Loh YC, Tan CS, Khadijah Adam S, Abdul Manan N, Basir R. General Pathways of Pain Sensation and the Major Neurotransmitters Involved in Pain Regulation. *International journal of molecular sciences.* 2018;19(8):2164.

18. Mills SEE, Nicolson KP, Smith BH. Chronic pain: a review of its epidemiology and associated factors in population-based studies. *Br J Anaesth.* 2019;123(2):e273-e283.

19. Ji R-R, Berta T, Nedergaard M. Glia and pain: Is chronic pain a gliopathy? *Pain.* 2013;154(0 1):S10-S28.

20. Cairns BE, Arendt-Nielsen L, Sacerdote P. Perspectives in Pain Research 2014: Neuroinflammation and glial cell activation: The cause of transition from acute to chronic pain? *Scandinavian Journal of Pain.* 2015;6:3-6.

21. Cui Y, Chen Y, Zhi J-L, Guo R-X, Feng J-Q, Chen P-X. Activation of p38 mitogen-activated protein kinase in spinal microglia mediates morphine antinociceptive tolerance. *Brain Research.* 2006;1069(1):235-243.

22. Guan J, Tanaka S, Kawakami K. Anticonvulsants or Antidepressants in Combination Pharmacotherapy for Treatment of Neuropathic Pain in Cancer Patients: A Systematic Review and Meta-analysis. *The Clinical journal of pain.* 2016;32(8):719-725.

23. Kalso E, Edwards JE, Moore RA, McQuay HJ. Opioids in chronic non-cancer pain: systematic review of efficacy and safety. *Pain.* 2004;112(3):372-380.

24. Ballantyne JC. Opioids for the Treatment of Chronic Pain: Mistakes Made, Lessons Learned, and Future Directions. *Anesth Analg.* 2017;125(5):1769-1778.

25. Kao S-C, Zhao X, Lee C-Y, et al. Absence of mu opioid receptor mRNA expression in astrocytes and microglia of rat spinal cord. *Neuroreport.* 2012;23(6):378-384.

26. Vukojević V, Ming Y, D'Addario C, et al. μ-Opioid receptor activation in live cells. *The FASEB Journal.* 2008;22(10):3537-3548.

27. Gurevich VV, Gurevich EV. Molecular Mechanisms of GPCR Signaling: A Structural Perspective. *Int J Mol Sci.* 2017;18(12).

28. Gurevich VV, Gurevich EV. GPCR Signaling Regulation: The Role of GRKs and Arrestins. *Front Pharmacol.* 2019;10:125.

29. Erlandson SC, McMahon C, Kruse AC. Structural Basis for G Protein–Coupled Receptor Signaling. *Annual Review of Biophysics.* 2018;47(1):1-18.

30. Wacker D, Stevens RC, Roth BL. How Ligands Illuminate GPCR Molecular Pharmacology. *Cell.* 2017;170(3):414-427.

31. Roth BL, Irwin JJ, Shoichet BK. Discovery of new GPCR ligands to illuminate new biology. *Nat Chem Biol.* 2017;13(11):1143-1151.

32. Weis WI, Kobilka BK. The Molecular Basis of G Protein–Coupled Receptor Activation. *Annual Review of Biochemistry.* 2014;87(1):897-919.

33. Roth S, Kholodenko BN, Smit MJ, Bruggeman FJ. G Protein-Coupled Receptor Signaling Networks from a Systems Perspective. *Mol Pharmacol.* 2015;88(3):604-616.

34. Ghelardini C, Di Cesare Mannelli L, Bianchi E. The pharmacological basis of opioids. *Clinical Cases in Mineral and Bone Metabolism.* 2015;12(3):219-221.

35. Traynor J. μ-Opioid receptors and regulators of G protein signaling (RGS) proteins: from a symposium on new concepts in mu-opioid pharmacology. *Drug and alcohol dependence.* 2012;121(3):173-180.

36. Alt A, Clark MJ, Woods JH, Traynor JR. Mu and Delta opioid receptors activate the same G proteins in human neuroblastoma SH-SY5Y cells. *British journal of pharmacology.* 2002;135(1):217-225.

37. Kuhar JR, Bedini A, Melief EJ, Chiu Y-C, Striegel HN, Chavkin C. Mu opioid receptor stimulation activates c-Jun N-terminal kinase 2 by distinct arrestin-dependent and independent mechanisms. *Cellular signalling.* 2015;27(9):1799-1806.

38. Darcq E, Kieffer BL. Opioid receptors: drivers to addiction? *Nat Rev Neurosci.* 2018;19(8):499-514.

39. Matthes HW, Maldonado R, Simonin F, et al. Loss of morphine-induced analgesia, reward effect and withdrawal symptoms in mice lacking the mu-opioid-receptor gene. *Nature.* 1996;383(6603):819-823.

40. Liu J-G, Prather PL. Chronic Exposure to μ-Opioid Agonists Produces Constitutive Activation of μ-Opioid Receptors in Direct Proportion to the Efficacy of the Agonist Used for Pretreatment. *Molecular Pharmacology.* 2001;60(1):53-62.

41. Cussac D, Rauly-Lestienne I, Heusler P, et al. μ-Opioid and 5-HT1A receptors heterodimerize and show signalling crosstalk via G protein and MAP-kinase pathways. *Cellular signalling.* 2012;24(8):1648-1657.

42. Corder G, Tawfik VL, Wang D, et al. Loss of mu opioid receptor signaling in nociceptors, but not microglia, abrogates morphine tolerance without disrupting analgesia. *Nat Med.* 2017;23(2):164-173.

43. Tsai RY, Tai YH, Tzeng JI, et al. ULTRA-LOW DOSE NALOXONE RESTORES THE ANTINOCICEPTIVE EFFECT OF MORPHINE IN PERTUSSIS TOXIN-TREATED RATS AND PREVENTS GLUTAMATE TRANSPORTER DOWNREGULATION BY SUPPRESSING THE p38 MITOGEN-ACTIVATED PROTEIN KINASE SIGNALING PATHWAY. *Neuroscience.* 2009;159(4):1244-1256.

44. Unterwald EM, Rubenfeld JM, Imai Y, Wang JB, Uhl GR, Kreek MJ. Chronic opioid antagonist administration upregulates mu opioid receptor binding without altering mu opioid receptor mRNA levels. *Brain Res Mol Brain Res.* 1995;33(2):351-355.

45. Toll L, Bruchas MR, Calo G, Cox BM, Zaveri NT. Nociceptin/Orphanin FQ Receptor Structure, Signaling, Ligands, Functions, and Interactions with Opioid Systems. *Pharmacological reviews.* 2016;68(2):419-457.

46. Derouiche L, Massotte D. G protein-coupled receptor heteromers are key players in substance use disorder. *Neurosci Biobehav Rev.* 2019;106:73-90.

47. Erbs E, Faget L, Scherrer G, et al. A mu–delta opioid receptor brain atlas reveals neuronal co-occurrence in subcortical networks. *Brain structure & function.* 2015;220.

48. Lam R, Gondin AB, Canals M, et al. Fluorescently Labeled Morphine Derivatives for Bioimaging Studies. *J Med Chem.* 2018;61(3):1316-1329.

49. Burns JA, Kroll DS, Feldman DE, et al. Molecular Imaging of Opioid and Dopamine Systems: Insights Into the Pharmacogenetics of Opioid Use Disorders. *Frontiers in Psychiatry.* 2019;10:626.

50. Polter AM, Li X. 5-HT1A receptor-regulated signal transduction pathways in brain. *Cellular signalling.* 2010;22(10):1406-1412.

51. Zimmer L, Descarries L. Internalization of serotonin 5-HT1A autoreceptors as an imaging biomarker of antidepressant response. *Wiley Interdisciplinary Reviews: Membrane Transport and Signaling.* 2012;1(3):239-245.

52. Barnes NM, Sharp T. A review of central 5-HT receptors and their function. *Neuropharmacology.* 1999;38(8):1083-1152.

53. Celada P, Bortolozzi A, Artigas F. Serotonin 5-HT1A receptors as targets for agents to treat psychiatric disorders: rationale and current status of research. *CNS Drugs.* 2013;27(9):703-716.

54. Loane C, Politis M. Buspirone: what is it all about? *Brain Res.* 2012;1461:111-118.

55. Eison AS, Temple DL. Buspirone: review of its pharmacology and current perspectives on its mechanism of action. *The American Journal of Medicine.* 1986;80(3):1-9.

56. Mahmood I, Sahajwalla C. Clinical Pharmacokinetics and Pharmacodynamics of Buspirone, an Anxiolytic Drug. *Clinical Pharmacokinetics.* 1999;36(4):277-287.

57. Zheng W, Li XH, Cai DB, et al. Adjunctive azapirone for schizophrenia: A meta-analysis of randomized, double-blind, placebo-controlled trials. *Eur Neuropsychopharmacol.* 2018;28(1):149-158.

58. Moret C. Combination/augmentation strategies for improving the treatment of depression. *Neuropsychiatric Disease and Treatment.* 2005;1(4):301-309.

59. Hofmann B, Afzelius P, Iversen J, et al. Buspirone, a serotonin receptor agonist, increases CD4 T-cell counts and modulates the immune system in HIV-seropositive subjects. *Aids.* 1996;10(12):1339-1347.

60. Leggio GM, Camillieri G, Platania CB, et al. Dopamine D3 receptor is necessary for ethanol consumption: an approach with buspirone. *Neuropsychopharmacology.* 2014;39(8):2017-2028.

61. Nayebi AM, Rezazadeh H, Nourafkan M. Buspirone attenuates tolerance to analgesic effect of morphine in mice with skin cancer. *Pak J Pharm Sci.* 2010;23(2):201-206.

62. Massotte D. In vivo opioid receptor heteromerization: where do we stand? *Br J Pharmacol.* 2015;172(2):420-434.

63. Haleem DJ. Serotonin-1A receptor dependent modulation of pain and reward for improving therapy of chronic pain. *Pharmacol Res.* 2018;134:212-219.

64. Gerits N, Kostenko S, Shiryaev A, Johannessen M, Moens U. Relations between the mitogen-activated protein kinase and the cAMP-dependent protein kinase pathways: comradeship and hostility. *Cell Signal.* 2008;20(9):1592-1607.

65. Tour J, Lofgren M, Mannerkorpi K, et al. Gene-to-gene interactions regulate endogenous pain modulation in fibromyalgia patients and healthy controls-antagonistic effects between opioid and serotonin-related genes. *Pain.* 2017;158(7):1194-1203.

66. Kosek E, Jensen KB, Lonsdorf TB, Schalling M, Ingvar M. Genetic variation in the serotonin transporter gene (5-HTTLPR, rs25531) influences the analgesic response to the short acting opioid Remifentanil in humans. *Molecular pain.* 2009;5:37-37.

67. Haleem DJ, Nawaz S. Inhibition of Reinforcing, Hyperalgesic, and Motor Effects of Morphine by Buspirone in Rats. *J Pain.* 2017;18(1):19-28.

68. Colpaert FC, Deseure K, Stinus L, Adriaensen H. High-efficacy 5-hydroxytryptamine 1A receptor activation counteracts opioid hyperallodynia and affective conditioning. *J Pharmacol Exp Ther.* 2006;316(2):892-899.

69. Xu XJ, Colpaert F, Wiesenfeld-Hallin Z. Opioid hyperalgesia and tolerance versus 5-HT1A receptor-mediated inverse tolerance. *Trends Pharmacol Sci.* 2003;24(12):634-639.

70. Rojas-Corrales MO, Berrocoso E, Mico JA. Role of 5-HT1A and 5-HT1B receptors in the antinociceptive effect of tramadol. *Eur J Pharmacol.* 2005;511(1):21-26.

71. Mico JA, Berrocoso E, Ortega-Alvaro A, Gibert-Rahola J, Rojas-Corrales MO. The role of 5-HT1A receptors in research strategy for extensive pain treatment. *Curr Top Med Chem.* 2006;6(18):1997-2003.

72. Marks DM, Shah MJ, Patkar AA, Masand PS, Park G-Y, Pae C-U. Serotonin-Norepinephrine Reuptake Inhibitors for Pain Control: Premise and Promise. *Current Neuropharmacology.* 2009;7(4):331-336.

73. Morgan D, Picker MJ. Discriminative stimulus effects of the 5HT1A agonist 8-OH-DPAT: attenuation by mu but not by kappa opioids. *Psychopharmacology (Berl).* 1995;122(4):336-345.

74. Rajdev P, Ghosh S. Fluorescence Resonance Energy Transfer (FRET): A Powerful Tool for Probing Amphiphilic Polymer Aggregates and Supramolecular Polymers. *The Journal of Physical Chemistry B.* 2019;123(2):327-342.

75. Elson Elliot L. Fluorescence Correlation Spectroscopy: Past, Present, Future. *Biophysical Journal.* 2011;101(12):2855-2870.

76. Vukojević V, Ming Y, D'Addario C, Rigler R, Johansson B, Terenius L. Ethanol/Naltrexone Interactions at the mu-Opioid Receptor. CLSM/FCS Study in Live Cells. *PLOS ONE.* 2008;3(12):e4008.

77. Kim SA, Heinze KG, Schwille P. Fluorescence correlation spectroscopy in living cells. *Nat Meth.* 2007;4(11):963-973.

78. Krieger JW, Singh AP, Bag N, et al. Imaging fluorescence (cross-) correlation spectroscopy in live cells and organisms. *Nat Protocols.* 2015;10(12):1948-1974.

79. Schwille P, Ries J. Principles and Applications of Fluorescence Correlation Spectroscopy (Fcs). *Biophotonics: Spectroscopy, Imaging, Sensing, and Manipulation.* 2011:63-85.

80. Tian Y, Martinez MM, Pappas D. Fluorescence Correlation Spectroscopy: A Review of Biochemical and Microfluidic Applications. *Applied Spectroscopy.* 2011;65(4):115A-115A.

81. Kim SA, Heinze KG, Schwille P. Fluorescence correlation spectroscopy in living cells. *Nat Methods.* 2007;4(11):963-973.

82. Ries J, Schwille P. Fluorescence correlation spectroscopy. *Bioessays.* 2012;34(5):361-368.

83. Schwille P. Fluorescence correlation spectroscopy and its potential for intracellular applications. *Cell Biochemistry and Biophysics.* 2001;34(3):383-408.

84. Day RN, Davidson MW. The fluorescent protein palette: tools for cellular imaging. *Chemical Society reviews.* 2009;38(10):2887-2921.

85. Bacia K, Petrášek Z, Schwille P. Correcting for Spectral Cross-Talk in Dual-Color Fluorescence Cross-Correlation Spectroscopy. *Chemphyschem.* 2012;13(5):1221-1231.

86. Chowdhury PK. FLUORESCENCE CORRELATION SPECTROSCOPY: A BRIEF REVIEW OF TECHNIQUES AND APPLICATIONS TO BIOMOLECULES AND BIOSYSTEMS. *2013.* 2013;2(2).

87. Du Z, Yu J, Li F, et al. In Situ Monitoring of p53 Protein and MDM2 Protein Interaction in Single Living Cells Using Single-Molecule Fluorescence Spectroscopy. *Anal Chem.* 2018;90(10):6144-6151.

88. Jonkman J, Brown CM. Any Way You Slice It—A Comparison of Confocal Microscopy Techniques. *Journal of Biomolecular Techniques : JBT.* 2015;26(2):54-65.

89. Weeks DSER. Confocal Microscopy. *Encyclopedia of Biomaterials and Biomedical Engineering*2005.

90. Long BR, Robinson DC, Zhong H. Subdiffractive microscopy: techniques, applications, and challenges. *Wiley interdisciplinary reviews Systems biology and medicine.* 2014;6(2):151-168.

91. Vangindertael J, Camacho R, Sempels W, Mizuno H, Dedecker P, Janssen KPF. An introduction to optical super-resolution microscopy for the adventurous biologist. *Methods Appl Fluoresc.* 2018;6(2):022003.

92. Gustafsson MG. Extended resolution fluorescence microscopy. *Curr Opin Struct Biol.* 1999;9(5):627-634.

93. Gustafsson MG. Surpassing the lateral resolution limit by a factor of two using structured illumination microscopy. *J Microsc.* 2000;198(Pt 2):82-87.

94. Yildiz A, Selvin PR. Fluorescence imaging with one nanometer accuracy: application to molecular motors. *Acc Chem Res.* 2005;38(7):574-582.

95. Wang Y, Cai E, Sheung J, Lee SH, Teng KW, Selvin PR. Fluorescence imaging with one-nanometer accuracy (FIONA). *J Vis Exp.* 2014(91):51774.

96. Hell SW, Wichmann J. Breaking the diffraction resolution limit by stimulated emission: stimulated-emission-depletion fluorescence microscopy. *Optics Letters.* 1994;19(11):780-782.

97. Leutenegger M, Ringemann C, Lasser T, Hell SW, Eggeling C. Fluorescence correlation spectroscopy with a total internal reflection fluorescence STED microscope (TIRF-STED-FCS). *Opt Express.* 2012;20(5):5243-5263.

98. Ettinger A, Wittmann T. Chapter 5 - Fluorescence live cell imaging. In: Jennifer CW, Torsten W, eds. *Methods in Cell Biology.* Vol Volume 123: Academic Press; 2014:77-94.

99. Liu Z, Lavis LD, Betzig E. Imaging live-cell dynamics and structure at the single-molecule level. *Molecular cell.* 2015;58(4):644-659.

100. Khan KH. Gene Expression in Mammalian Cells and its Applications. *Advanced Pharmaceutical Bulletin.* 2013;3(2):257-263.

101. Thomas P, Smart TG. HEK293 cell line: A vehicle for the expression of recombinant proteins. *Journal of Pharmacological and Toxicological Methods.* 2005;51(3):187-200.

102. Westerink RHS, Ewing AG. The PC12 cell as model for neurosecretion. *Acta Physiologica.* 2008;192(2):273-285.

103. Felgner PL, Gadek TR, Holm M, et al. Lipofection: a highly efficient, lipid-mediated DNA-transfection procedure. *Proceedings of the National Academy of Sciences of the United States of America.* 1987;84(21):7413-7417.

104. Lee JH, Ahn HH, Kim KS, et al. Polyethyleneimine-mediated gene delivery into rat pheochromocytoma PC-12 cells. *J Tissue Eng Regen Med.* 2008;2(5):288-295.

105. Hulme EC, Trevethick MA. Ligand binding assays at equilibrium: validation and interpretation. *Br J Pharmacol.* 2010;161(6):1219-1237.

106. Watabe M, Arjunan S, Chew W, Kaizu K, Takahashi K. *Cooperativity transitions driven by higher-order oligomer formations in ligand-induced receptor dimerization.* 2019.

107. McIntyre IM, Anderson DT. Postmortem Fentanyl Concentrations: A Review. *Journal of Forensic Research.* 2012;3(8):1-10.

108. Macey TA, Lowe JD, Chavkin C. Mu opioid receptor activation of ERK1/2 is GRK3 and arrestin dependent in striatal neurons. *The Journal of biological chemistry.* 2006;281(45):34515-34524.

109. Tan M, Walwyn WM, Evans CJ, Xie C-W. p38 MAPK and β-Arrestin 2 Mediate Functional Interactions between Endogenous μ-Opioid and α2A-Adrenergic Receptors in Neurons. *Journal of Biological Chemistry.* 2009;284(10):6270-6281.

110. Goldbeter A. *Biochemical Oscillations and Cellular Rhythms: The Molecular Bases of Periodic and Chaotic Behaviour.* Cambridge: Cambridge University Press; 1996.

111. Petersen J, Wright SC, Rodríguez D, et al. Agonist-induced dimer dissociation as a macromolecular step in G protein-coupled receptor signaling. *Nature Communications.* 2017;8(1):226.

112. Foster SR, Bräuner-Osborne H. Investigating Internalization and Intracellular Trafficking of GPCRs: New Techniques and Real-Time Experimental Approaches. In: Ulloa-Aguirre A, Tao Y-X, eds. *Targeting Trafficking in Drug Development.* Cham: Springer International Publishing; 2018:41-61.

113. Kasai RS, Kusumi A. Single-molecule imaging revealed dynamic GPCR dimerization. *Current Opinion in Cell Biology.* 2014;27:78-86.

114. Christrup LL, Foster D, Popper LD, Troen T, Upton R. Pharmacokinetics, efficacy, and tolerability of fentanyl following intranasal versus intravenous administration in adults undergoing third-molar extraction: a randomized, double-blind, double-dummy, two-way, crossover study. *Clin Ther.* 2008;30(3):469-481.

115. Trescot AM. Review of the role of opioids in cancer pain. *J Natl Compr Canc Netw.* 2010;8(9):1087-1094.

116. Pereira J, Lawlor P, Vigano A, Dorgan M, Bruera E. Equianalgesic dose ratios for opioids. a critical review and proposals for long-term dosing. *J Pain Symptom Manage.* 2001;22(2):672-687.

117. Rennick A, Atkinson T, Cimino NM, Strassels SA, McPherson ML, Fudin J. Variability in Opioid Equivalence Calculations. *Pain Med.* 2016;17(5):892-898.

118. Yue QY, Hasselström J, Svensson JO, Säwe J. Pharmacokinetics of codeine and its metabolites in Caucasian healthy volunteers: comparisons between extensive and poor hydroxylators of debrisoquine. *British journal of clinical pharmacology.* 1991;31(6):635-642.

119. Cortazzo MH, Copenhaver D, Fishman SM. 36 - Major Opioids and Chronic Opioid Therapy. In: Benzon HT, Rathmell JP, Wu CL, Turk DC, Argoff CE, Hurley RW, eds. *Practical Management of Pain (Fifth Edition).* Philadelphia: Mosby; 2014:495-507.e493.

120. Samuels BA, Nautiyal KM, Kruegel AC, et al. The Behavioral Effects of the Antidepressant Tianeptine Require the Mu-Opioid Receptor. *Neuropsychopharmacology.* 2017.

121. Mignat C, Wille U, Ziegler A. Affinity profiles of morphine, codeine, dihydrocodeine and their glucuronides at opioid receptor subtypes. *Life Sci.* 1995;56(10):793-799.

122. Schmidt H, Vormfelde S, Klinder K, et al. Affinities of dihydrocodeine and its metabolites to opioid receptors. *Pharmacol Toxicol.* 2002;91(2):57-63.

123. Ingelman-Sundberg M. Genetic polymorphisms of cytochrome P450 2D6 (CYP2D6): clinical consequences, evolutionary aspects and functional diversity. *The Pharmacogenomics Journal.* 2005;5(1):6-13.

124. Sibille KT, Bartsch F, Reddy D, Fillingim RB, Keil A. Increasing Neuroplasticity to Bolster Chronic Pain Treatment: A Role for Intermittent Fasting and Glucose Administration? *The journal of pain : official journal of the American Pain Society.* 2016;17(3):275-281.

125. Jasmin L, Wu MV, Ohara PT. GABA puts a stop to pain. *Curr Drug Targets CNS Neurol Disord.* 2004;3(6):487-505.

126. Korneeva NL, Schrott LM. Chronic oxycodone exposure alters translational and signaling pathways in the rat brain stem. *The FASEB Journal.* 2011;25(1_supplement):lb414-lb414.

127. Hutchinson MR, Northcutt AL, Hiranita T, et al. Opioid Activation of Toll-Like Receptor 4 Contributes to Drug Reinforcement. *The Journal of Neuroscience.* 2012;32(33):11187.

128. Al-Hasani R, Bruchas MR. Molecular mechanisms of opioid receptor-dependent signaling and behavior. *Anesthesiology.* 2011;115(6):1363-1381.

129. Remillard D, Kaye AD, McAnally H. Oxycodone's Unparalleled Addictive Potential: Is it Time for a Moratorium? *Curr Pain Headache Rep.* 2019;23(2):15.

130. Valjent E, Pages C, Herve D, Girault JA, Caboche J. Addictive and non-addictive drugs induce distinct and specific patterns of ERK activation in mouse brain. *Eur J Neurosci.* 2004;19(7):1826-1836.

131. Duraffourd C, Kumala E, Anselmi L, Brecha NC, Sternini C. Opioid-induced mitogen-activated protein kinase signaling in rat enteric neurons following chronic morphine treatment. *PLoS One.* 2014;9(10):e110230.

132. Macey TA, Lowe JD, Chavkin C. Mu opioid receptor activation of ERK1/2 is GRK3 and arrestin dependent in striatal neurons. *J Biol Chem.* 2006;281(45):34515-34524.

133. Reyes-Gibby CC, Yuan C, Wang J, Yeung SC, Shete S. Gene network analysis shows immune-signaling and ERK1/2 as novel genetic markers for multiple addiction phenotypes: alcohol, smoking and opioid addiction. *BMC Syst Biol.* 2015;9:25.

134. Paul ML, Graybiel AM, David JC, Robertson HA. D1-like and D2-like dopamine receptors synergistically activate rotation and c-fos expression in the dopamine-depleted striatum in a rat model of Parkinson's disease. *The Journal of Neuroscience.* 1992;12(10):3729.

135. Prasanna X, Jafurulla M, Sengupta D, Chattopadhyay A. The ganglioside GM1 interacts with the serotonin1A receptor via the sphingolipid binding domain. *Biochim Biophys Acta.* 2016;1858(11):2818-2826.

136. Alpaugh M, Galleguillos D, Forero J, et al. Disease-modifying effects of ganglioside GM1 in Huntington's disease models. *EMBO Mol Med.* 2017;9(11):1537-1557.

137. Shin J, Yin Y, Park H, et al. p38 siRNA-encapsulated PLGA nanoparticles alleviate neuropathic pain behavior in rats by inhibiting microglia activation. *Nanomedicine (Lond).* 2018;13(13):1607-1621.

138. Jez M, Bas T, Veber M, et al. The hazards of DAPI photoconversion: effects of dye, mounting media and fixative, and how to minimize the problem. *Histochem Cell Biol.* 2013;139(1):195-204.

139. Bertelsen M. [20] - Multiplex Analysis of Inflammatory Signaling Pathways Using a High-Content Imaging System. In: Inglese J, ed. *Methods in Enzymology.* Vol 414: Academic Press; 2006:348-363.

140. Kasai RS, Suzuki KG, Prossnitz ER, et al. Full characterization of GPCR monomer-dimer dynamic equilibrium by single molecule imaging. *J Cell Biol.* 2011;192(3):463-480.

9 PAPERS